

Prediction of Ripple Properties in Shelf Seas

Mark 1 Predictor

**R L Soulsby
RJS Whitehouse**

**Report TR 150
Release 1.1
February 2005**



Document Information

| | |
|------------------------------|--|
| Project | Prediction of Ripple Properties in Shelf Seas |
| Report title | Mark 1 Predictor |
| Client | U.S. Office of Naval Research |
| Client Representative | Dr Thomas Drake |
| Project No. | CBR3689 |
| Report No. | TR 150 |
| Doc. ref. | TR150-Prediction of Ripple Properties in Shelf Seas rel1-1.doc |
| Project Manager | Prof. Richard Soulsby |
| Project Sponsor | Dr Richard Whitehouse |

Document History

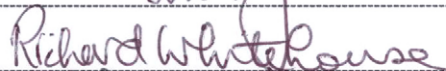
| Date | Release | Prepared | Approved | Authorised | Notes |
|----------|---------|----------|----------|------------|-----------------|
| 28/02/05 | 1.0 | rls | rjsw | kap | Interim version |
| 04/03/05 | 1.1 | rls | rjsw | kap | Revised version |

Prepared

Approved

Authorised







© HR Wallingford Limited

This report is a contribution to research generally and it would be imprudent for third parties to rely on it in specific applications without first checking its suitability. Various sections of this report rely on data supplied by or drawn from third party sources. HR Wallingford accepts no liability for loss or damage suffered by the client or third parties as a result of errors or inaccuracies in such third party data. HR Wallingford will only accept responsibility for the use of its material in specific projects where it has been engaged to advise upon a specific commission and given the opportunity to express a view on the reliability of the material for the particular applications.

Summary

Prediction of Ripple Properties in Shelf Seas

Mark 1 Predictor

R L Soulsby
RJS Whitehouse

Report TR 150
February 2005

The work under this contract is intended to transfer European data and thinking about sea-bed ripples into the ONR Ripples DRI program. The goal is to develop a generic predictor for bedform existence, growth/decay, height and spacing, and temporal variability at a sandy seabed location (ripples in currents, waves, and waves-plus-currents) as a function of: sediment characteristics, water depth, wave and current forcing, biological effects and time history of these processes. The project makes use of existing data, through data mining and interpretation, to underpin the ongoing SAX99 and SAX04 collection of specific sediment-acoustic data within the ONR program. The present report relates to Phase 1 of the project, in which data was assembled, and a predictor for equilibrium ripple properties developed.

Discussions have been held with researchers working on ripples in the UK, Netherlands and Italy. Recent (not yet published) work on determining the types of bedform expected for given wave and current conditions has been summarised. A number of other European sources are summarised, highlighting their contributions to knowledge or data on ripples. A data-set has been assembled comprising 3,098 entries from 51 sources, approximately 75% of which are European. In 2,460 cases either height or wavelength of bedforms were quoted, and 1,751 relate to ripples. The remainder relate to other types of bedform, or plane bed, or (in some cases) there was no bedform information. Statistical data on the heights and wavelengths of the ripples in the data-set have been derived, including frequency distributions subdivided by flow classification. The percentiles of exceedance of ripple heights and wavelengths have been derived, subdivided by grain-size as well as flow classification. A formula with two free coefficients expressing the height and wavelength as functions of grain-size has been calibrated against all the percentile results. A further analysis to incorporate the dependence on wave and/or current conditions will follow. The 50-percentile (median) heights and wavelengths are regarded as the typical values under *all* flow conditions, whereas the 90-percentile are regarded as the equilibrium values for the flow conditions at which maximum values are reached. An Excel spreadsheet has been devised to display a contour plot of the bed elevations in an area of sea-bed a few metres square, together with cross-sections through the bed, for wave ripples. A more refined version will follow. A number of items of work will be completed before the SAX 04 workshop in May 2005.

Acknowledgements

We gratefully acknowledge the contributions made by our European colleagues Maarten Kleinhans, Bart Grasmeijer, Carl Amos, John Harris, Leo van Rijn and Enrico Foti. Maarten Kleinhans kindly made his data-set of bedform properties available to us, in the context of the EU collaborative project SANDPIT (Contract No. EVK3-2001-00056). The data-base compiled during the EU collaborative research project SEDMOC (Contract No. MAS3-CT97-0115) was also made use of. We are grateful to Dr Christine Lauchlan and Dr Sanne Niemann for undertaking much of the computational work in the present project.

Contents

| | |
|-----------------------------|------------|
| <i>Title page</i> | <i>i</i> |
| <i>Document Information</i> | <i>ii</i> |
| <i>Summary</i> | <i>iii</i> |
| <i>Acknowledgements</i> | <i>v</i> |
| <i>Contents</i> | <i>vii</i> |

| | | |
|-----|---|----|
| 1. | Introduction | 1 |
| 1.1 | ONR BAA 04-001 | 1 |
| 1.2 | Objectives | 1 |
| 1.3 | Background..... | 2 |
| 2. | Behaviour of sea-bed ripples | 3 |
| 2.1 | Ripples and sonar propagation | 3 |
| 2.2 | Current-generated ripples | 4 |
| 2.3 | Wave-generated ripples | 5 |
| 2.4 | Wave-plus-current ripples | 6 |
| 3. | Bedform existence diagrams | 6 |
| 4. | Sources of data on ripple dimensions | 8 |
| 4.1 | Current ripples | 9 |
| 4.2 | Wave ripples | 11 |
| 4.3 | Wave-plus-current ripples | 12 |
| 5. | New predictor for ONR applications (Mark 1) | 14 |
| 5.1 | Aims of predictor..... | 14 |
| 5.2 | Existing predictors..... | 14 |
| 5.3 | Analysis and interpretation of data-set | 15 |
| 5.4 | Ripple height | 16 |
| 5.5 | Ripple spacing | 16 |
| 5.6 | Ripple orientation | 17 |
| 5.7 | Ripple shape | 17 |
| 5.8 | Contour plots | 18 |
| 6. | Tests against existing data | 18 |
| 7. | Tests against SAX 99 data | 19 |
| 8. | Proposed work in Phase 2 | 19 |
| 9. | Conclusions | 19 |
| 10. | References and Bibliography | 21 |

Tables

| | |
|---------|--|
| Table 1 | Summary of percentiles of ripple height and wavelength subdivided by grain size |
| Table 2 | Tentative bed state definitions proposed by Kleinhans. <i>Reproduced from Kleinhans (2005) with permission</i> |
| Table 3 | Summary of data sources and types of data available |

Contents continued

| | |
|---------|---|
| Table 4 | Classification of available data |
| Table 5 | Coefficients a and b in ripple height and wavelength predictors |

Figures

| | |
|-----------|---|
| Figure 1 | Bedform existence diagram for waves plus currents using Shields' parameters proposed by Kleinhans, based on rational criteria for beginning of motion and sheetflow/USPB (here plotted for $D=0.21$ mm) |
| Figure 2 | Normalised bed state diagram based on rational criteria for beginning of motion and sheetflow/UPB |
| Figure 3 | Frequency distribution of <i>all</i> ripple heights |
| Figure 4 | Frequency distribution of <i>all</i> ripple wavelengths < 4 m |
| Figure 5 | Frequency distribution of ripple heights subdivided into flow classes |
| Figure 6 | Frequency distribution of ripple wavelengths (< 4 m) subdivided into flow classes |
| Figure 7 | Frequency distribution of ripple heights subdivided into lab and field experiments |
| Figure 8 | Frequency distribution of ripple wavelengths (< 4 m) subdivided into lab and field experiments |
| Figure 9 | 50 and 90-percentile ripple heights for currents, with fitted prediction curves |
| Figure 10 | 50 and 90-percentile ripple heights for waves, with fitted prediction curves |
| Figure 11 | 50 and 90-percentile ripple heights for $W + C$, with fitted prediction curves |
| Figure 12 | 50 and 90-percentile ripple wavelengths (< 1.5 m) for currents, with fitted prediction curves |
| Figure 13 | 50 and 90-percentile ripple wavelengths (< 1.5 m) for waves, with fitted prediction curves |
| Figure 14 | 50 and 90-percentile ripple wavelengths (< 1.5 m) for $W + C$, with fitted prediction curves |
| Figure 15 | Example of contour plot of bed elevation and cross-sections of wave-generated ripples for wave direction 30° , ripple wavelength 1.5m, ripple height 0.4m, sharpness factor = 0.5 |
| Figure 16 | Example of contour plot of bed elevation and cross-sections of wave-generated ripples for wave direction 60° , ripple wavelength 2m, ripple height 0.4m, sharpness factor = 0.1 |

1. *Introduction*

1.1 ONR BAA 04-001

This project has the title “Development of a new marine ripple bedform predictor for application in sandy shelf environments”. It forms part of the Department Research Initiative (DRI), ONR, on Critical Benthic Environmental Processes and Modeling at SAX04 (aka Ripples DRI). It refers to the ONR Long Range BAA 04-001, dated 10 Sep 2003.

1.2 OBJECTIVES

The goal is to develop a generic predictor for bedform existence, growth/decay, height and spacing, and temporal variability at a sandy seabed location (ripples in currents, ripples in waves, ripples in waves and currents) as a function of:

- sediment characteristics
- water depth
- wave and current forcing
- biological effects
- time history of the above processes.

The research makes use of the knowledge of marine sediment transport bedform prediction held by the PIs and accessed in the UK/European framework to the DRI program. The project makes use of existing data, through data mining and interpretation, to underpin the ongoing SAX99 and SAX04 collection of specific sediment-acoustic data within the ONR program. A Mark 1 version of the ripple predictor will be developed initially based on this existing data. An improved Mark 2 predictor will be developed later in the project using (and tested against) the data from the SAX04 program. The resulting algorithm will be delivered for use in the DRI Ripples program.

The project will provide predictive tools for the response of ripples to changes in wave and wave-current forcing, comment on rates of biological degradation, include the effects of grain size, density and cohesion, and show how these affect surface and subsurface sedimentary structures.

The present report relates to the Phase 1 objectives, specifically:

- Assemble data, model results and knowledge from our own sources, plus European, North American and international sources, on ripples and larger bedforms.
- Devise parameterisations for predicting ripple height, spacing and orientation as functions of local, instantaneous input variables of water depth, current speed, wave characteristics, sediment properties, based on our own library of data.
- Delivery of Mark 1 ripple predictor for above output quantities.

The form of the ripple predictor should be geared to its effect on sonar performance, and written in a form that could be used to give a forecast of the spatial and temporal variations of ripple properties over a sea area, as a function of hydrodynamic and sedimentary input distributions.

1.3 BACKGROUND

We distinguish *ripples* as small-scale bedforms, having spacing of order 1m and heights of order 0.1m, which enhance the penetration of sonar signals into the subsurface. We also consider the larger bedforms on the seabed, such as *mega-ripples*, *dunes* and *sandwaves*, with spacings from a few metres to 100s of metres and heights from about 0.5m to several metres, which can affect the burial of mines. Our attention is mainly focussed on the ripples, but with some attention also to the larger features.

The approach is based primarily on data mining, generating meaningful physics-based empirically-calibrated bedform predictors. This will be supported by numerical simulation of bedform parameters with both spatial and temporal variation. Over the last 10 years the investigators have collected together a substantial database of references and data sources on the topic of bedforms in coastal and shelf waters. This includes our own data from a wide range of shelf-seas and estuarine sources, together with laboratory experiments.

The PIs have undertaken collaborative research that relates to ripples within the following collaborative research projects, which we have drawn upon for data and discussion with other EU researchers within the compass of this Phase 1 Ripples DRI work:

- **COAST3D (1997-2001).** A large EU-funded collaborative research project (11 partners in 5 countries), undertaking collection of field data on near-bed hydrodynamics, sediment dynamics and morphodynamics at contrasting sites in the Netherlands and UK.
- **SEDMOC (1998-2001).** An EU-funded collaborative research project to advance understanding of coastal sand transport, and develop improved predictors.
- **SANDPIT (2002-2005).** An EU-funded project to advance understanding of the behaviour of offshore sand mining pits and their effects on the seabed and coastline, and develop improved predictors.
- **EstProc (2002-2004).** A UK government funded collaborative research project (partners in UK and Netherlands) researching physical and biological processes affecting hydrodynamics, sediment dynamics and morphodynamics in estuaries.

We have had discussions, and in some cases received data from, the following individuals in connection with the present project:

- Maarten Kleinhans and Bart Grasmeijer (Utrecht University, NL)
- Carl Amos (Southampton University, UK)
- John Harris (Associated British Ports marine environmental research, UK)
- Leo van Rijn (Delft Hydraulics, NL)
- Enrico Foti (University of Catania, IT).

We are grateful to all of the above for giving their time to assist the project.

2. *Behaviour of sea-bed ripples*

2.1 RIPPLES AND SONAR PROPAGATION

The behaviour of ripples (or other types of bedform), as they might affect sonar propagation, can be considered in three stages:

1. Prediction of the *existence* of different types of bedform under different hydrodynamic conditions (waves, currents, water depths) and sedimentary conditions (characteristic grain-sizes, density, mineralogy).
2. Prediction of the characteristic descriptors of ripples *in equilibrium* with the hydrodynamic conditions (i.e. assuming that the conditions have lasted sufficiently long and been sufficiently constant that the ripples have evolved fully).
3. Prediction of the characteristic descriptors of ripples in conditions that are *not in equilibrium*, and how fast they respond (tidally varying currents, wind-driven varying currents, varying waves in storms, biological effects).

Phase 1 of the project considers items 1 and 2, and Phase 2 considers item 3.

The term *bedform* is used here to encompass any kind of deviation from a flat bed, of which ripples are the most prevalent, but can also include dunes, mega-ripples, hummocks and sandwaves. These are discussed further in Chapter 3. Ripples (and other bedforms) may be *two-dimensional* (2D), in which case the ripple crests form straight or gently waving lines that are very much longer than the wavelength (i.e. spacing perpendicular to the crest-line), or three-dimensional (3D), in which case the shape of an individual ripple can be traced (along the crest-line) for only a short distance. Both 2D and 3D ripples (and bedforms) are encountered on the sea-bed, but their effects on sonar propagation will be different.

We consider the following properties of ripples that might affect sonar propagation:

- height
- wavelength (i.e. spacing perpendicular to the crest-lines)
- crest-length (i.e. spacing along the crest-lines)
- orientation (with respect to the North, or sonar source)
- slope with respect to horizontal (as seen by sonar source)
- shape
- grain-size.

[We would appreciate feedback from ONR as to whether these are the quantities of interest.]

For each of these, the effect we might expect ripples to have on sonar are as follows:

- **height:** the sonar reflection or transmission will increase with ripple height.
- **spacing:** the interaction between ripples and sonar will depend on the relation between the sonar wavelength (projected onto the bed) and the spacing of the ripples, being strongest if these are matched. This interaction will be stronger if the periodicity of the ripples is “sharp” rather than diffuse.

- **crest-length:** long-crested (2D) ripples will have little impact on a sonar beam directed along the crest-line, whereas short-crested (3D) ripples will impact a sonar beam even if it is directed along the (less well-defined) crest-line.
- **orientation:** the strength of the interaction will be greatest if the sonar source faces the steepest slopes of the ripples directly (in azimuth), and will be progressively weaker as the ripple crest-lines form greater azimuths with the sonar direction.
- **slope:** the reflection/transmission of sonar will be greatest if the face of the ripple-slopes is most nearly perpendicular to the sonar beam. Hence asymmetric current-induced ripples will have greatest interaction with a sonar beam directed towards the steeper (lee) slope, and a weaker interaction if it is directed towards the gentler (stoss) slope.
- **shape:** reflection or transmission will be greater for sharp-crested (triangular) cross-section ripples than for round-crested ripples.
- **grain-size:** the absorption or reflection of sonar will also depend on the grain-size of the sediment forming the ripple.

[Again, we would appreciate feedback from ONR as to whether we have interpreted the interaction with sonar correctly.]

The following general properties of ripples are gleaned from many sources, plus personal experience at sea and in laboratories. The sources include: Sleath, 1984; Dyer, 1986; Fredsøe and Deigaard, 1992; Nielsen, 1992; Van Rijn, 1993; Soulsby, 1997.

2.2 CURRENT-GENERATED RIPPLES

Ripples are generated by currents in rivers, estuaries and the sea. The current must exceed the threshold of motion of the sediment to form ripples, but at times when currents are very weak (e.g. at slack water in tidal currents) ripples will remain from preceding stronger flows. The ripple travels slowly downstream (0.3 to 4mm/s), typically travelling through one wavelength in about 5 to 20 minutes. Current-generated ripples can respond relatively quickly to changes in current speed or direction, provided that the flow is strong, such as at spring tides. During neap tides, the ripples move weakly and only near the time of maximum current. The behaviour of ripples in tidal (or time-varying wind-driven) flows can be approximated by those found in steady flows, but there is always a time lag, so the ripples are rarely truly in equilibrium with the simultaneous flow conditions. Ripples can be found covering the surface of larger bedforms, such as dunes and sand-waves, as well as on their own.

- **height:** The ripple height is typically 8 to 33mm, with a median of 21mm (see Table 1). Under very strong flow conditions (greater than about 1.5m/s) the ripples are washed out to form an almost flat bed, known as Upper Stage Plane Bed, with the sand moving as Sheet Flow in a blanket a few millimetres to centimetres thick just above the bed. The ripple height gradually decreases with increasing current speed until this occurs.
- **wavelength:** The ripple wavelength is typically between 0.08 and 0.8m, with a median of 0.2m (see Table 1).
- **crest-length:** The ripples are usually 3D, with crest-lengths of about one to three wavelengths. Viewed from above, they form a randomly spaced pattern, but there is a tendency for the highest point of one ripple to lie immediately downstream of the valley between two upstream ripples. However, individual ripples vary strongly from each other (i.e. their periodicity is weak).

- **orientation:** The crest-line of the ripples is approximately at right-angles to the direction of the current (if the bed is horizontal). In a rotating tidal flow the direction of the ripple crests tries to follow the flow direction.
- **shape and slopes:** A cross-section through the ripple has a strongly asymmetric shape, with a steep down-stream facing (lee) slope of about 10° to 14° to the vertical (up to about 25° locally), and a gentler up-stream facing (stoss) slope of about 7° to 9° to the vertical (Whitehouse *et al* 1998a). In a recti-linear (to-and-fro) tidal current, the direction of the asymmetry reverses within one to two hours after the flow reverses, and the ripples then start to travel in the new direction of the current.
- **grain-size:** The wavelength and height of the ripples increase with the grain-diameter of the sediment they are formed in, but ripples do not form for sand of grain diameter larger than about 0.8mm. Likewise, well-defined ripples do not form if the sediment contains more than a few percent of silt or clay (diameters smaller than about 0.06mm) material.

2.3 WAVE-GENERATED RIPPLES

Waves generate ripples through the orbital velocities they produce at the sea bed. The orbital velocities increase with increasing wave height, increasing wave period, and decreasing water depth. As with currents, the orbital velocity must exceed the threshold of motion of the sediment to form ripples, but at times when the velocities are very weak (e.g. calm after a storm) ripples will remain from preceding stronger flows. The ripples can migrate, but less strongly than current ripples. They may migrate onshore in response to the asymmetry between the strong onshore velocity under the wave crests and the weaker offshore velocity under the wave troughs, or offshore if they are influenced by a rip current or undertow (although strictly they are then wave-plus-current ripples).

- **height:** The ripple height is typically 8 to 50mm, with a median of 20mm (see Table 1). Under very strong flow conditions the ripples are washed out to form an almost flat bed with wave-induced sheet-flow. The ripple height gradually decreases with increasing current speed until this occurs. The sheet flow can result in the bed being left with low hummock bedforms.
- **wavelength:** The ripple wavelength is typically between 0.07 and 0.55m, with a median of 0.15m (see Table 1). The wavelength is most closely related to the orbital diameter of the waves (the distance travelled by a water particle near the bed in half a wave period). However, it also increases with grain-size.
- **crest-length:** The ripples are usually two-dimensional, with straight or gently sinuous crests which sometimes merge. Hence crest-lengths are many times the wavelength.
- **orientation:** The crest-line of the ripples is approximately at right-angles to the direction of the wave propagation (if the bed is horizontal). If the wave direction changes, the direction of the ripple crests tries to follow the flow direction.
- **shape and slopes:** A cross-section through the ripple has a symmetrical shape, usually with a crest that is sharper than the trough. However, the sharpness decreases with increasing grain-size.
- **grain-size:** The wavelength and height of the ripples increase with the grain-diameter of the sediment they are formed in, but ripples do not form for sand of grain diameter larger than about 0.8mm. Likewise, well-defined ripples do not form if the sediment contains more than a few percent of silt or clay (diameters smaller than about 0.06mm) material.

2.4 WAVE-PLUS-CURRENT RIPPLES

Ripples generated by the combined effect of superimposed waves and currents (W+C) display some of the features of both current-alone and wave-alone ripples. In addition, the relative angle between the wave propagation direction and the current direction influences the ripple characteristics. If the wave travels parallel to the current (with it or against it, such as in estuaries) the ripple pattern is largely two-dimensional. If the waves travel perpendicular, or at a broad angle, to the current direction (typical of straight coastlines) the ripple pattern is generally three-dimensional.

For example, a weak current perpendicular to strong waves gives rise to predominantly 2D wave ripples, but with serpentine crests. Three classes of W+C ripples can be identified: wave-dominated, current-dominated, and mixed. Thus a weak current on strong waves produces a modulated form of wave-alone ripples, weak waves on a strong current produces a modulated form of current-alone ripples, while roughly equal forcing by waves and currents produces a complex mixed ripple pattern. This is illustrated further in Section 3. In general, most areas of shelf seas experience some combination of the effects of waves and currents.

3. *Bedform existence diagrams*

The first task in predicting ripple properties is to establish what kind of bedform will be present for given wave and current conditions, for a given water depth and sediment properties. This question, sometimes known as Phase Diagrams, or Bed States, has been tackled by many researchers, initially for rivers, then for waves, and most recently for combined current and waves. There are a number of overviews of these methods, for example papers by Allen (1984) and Southard and Boguchwal (1990) in the sedimentological literature, and books by Sleath (1984) and Van Rijn (1993). A very recent overview by Kleinhans (2005) is summarised here, since it draws on most of the earlier reviews.

A wide range of possible bedform types has been identified by researchers. Kleinhans (2005) lists (see Table 2 for descriptions):

- lower stage plane bed (below threshold of motion)
- upper stage plane bed (bedforms wiped out, sheet flow)
- upper flow regime, antidunes
- current ripples
- current dunes (2D and 3D)
- wave ripples
- hummocks
- mixed flow ripples (waves and currents combined)
- long wave ripples
- megaripples.

Since the plane bed cases are not strictly bedforms, the name “bed states” can be used to include them. To this list can be added sand-waves, at larger scales still.

Existence diagrams for *currents* alone show boundaries between the different current-generated bed states on plots of some measure of current speed versus some measure of grainsize. The current may be represented by the dimensional current speed (in which

case the water depth is another parameter), or the stream-power, or the Shields parameter (total or skin-friction), or the ratio of actual bed shear-stress to threshold bed shear-stress. The latter two are dimensionless parameters. The grainsize may be represented by plain median diameter d_{50} , the grain Reynolds number, or the dimensionless grain diameter D_* (or quantities closely related to it).

For present purposes we use the skin-friction (current-induced) Shields parameter:

$$\theta_c = \tau_c / [(\rho_s - \rho)gd_{50}] \quad (3.1)$$

and the dimensionless grain diameter D_* :

$$D_* = d_{50} [((s-1)g/\nu^2)]^{(1/3)} \quad (3.2)$$

since these are used by Kleinhans (2005).

Here τ_c is the current-induced bed shear-stress, ρ and ρ_s are the densities of water and sediment material respectively, $s = \rho_s/\rho$, ν is the kinematic viscosity of water, and g is the acceleration due to gravity.

Existence diagrams for *waves* alone show boundaries between the wave-generated bed states on plots of some measure of wave orbital velocity at the bed versus some measure of grainsize. The orbital velocity may be represented directly in dimensional terms, or by the wave mobility number, or the skin-friction (wave-induced) Shields parameter. The latter is defined by:

$$\theta_w = \tau_w / [(\rho_s - \rho)gd_{50}] \quad (3.3)$$

where τ_w is the amplitude of the wave-induced oscillatory shear-stress.

Existence diagrams for *combined waves and currents* thus strictly need boundaries plotted against three parameters: θ_c , θ_w and D_* . Kleinhans (2005) plotted an existence diagram, reproduced here as Figure 1, in terms of θ_c versus θ_w for a given grainsize of $d_{50} = 0.21\text{mm}$. He superimposed bedform types from data of Li and Amos (1998, 1999a, b). Essentially there are five main categories of bed state: no motion, sheet flow (upper stage plane bed), current ripples, wave ripples, and mixed (wave + current) ripples.

Kleinhans (2005) then extended the existence diagram to become more general for any grain-size by a normalisation procedure. A mobility parameter M was devised which postulates the Shields threshold of motion criterion at $\theta_c + \theta_w = \alpha$ and the onset of sheetflow at $\theta_c + \theta_w = \beta$:

$$M = [(\theta_i - \theta_{cr}) / (\theta_{sh} - \theta_{cr})](\beta - \alpha) + \alpha \quad (3.4)$$

in which θ_i = Shields parameter of an observation, θ_{sh} = shields parameter at which ripples are washed out and θ_{cr} = threshold shields parameter for sediment motion. The parameters $\alpha = 0.05$ and $\beta = 1$ are here conveniently chosen approximating the Shields criteria. The effect of normalisation is that observations plot in the appropriate stability field independently of grain size, which allows the direct comparison of the data for $0.03 < d < 40\text{mm}$ (Figure 2). This parameter set provides a framework within which other sheetflow or threshold of motion criteria can be tested as well.

4. Sources of data on ripple dimensions

For the purposes of the Ripples DRI project we have assembled a large set of data from a wide variety of sources. The data was assembled from two large European projects (SEDMOC and SANDPIT) which have created data-bases for general sand transport purposes, together with data from HR Wallingford and other sources we have access to. Altogether the data are drawn from 61 sources (see Table 3), of which about 75% are European researchers. Of these, 40 sources quote data specifically for ripples with either height or wavelength quoted.

A total of **3,098** data were examined and classified (Table 4). In terms of the types of bedforms observed:

- 1,751 represented ripples,
- 119 represented dunes,
- 19 represented megaripples,
- 228 represented a plane bed,
- and the remainder were either a different kind of bedform or were not specifically identified.

Many, but not all, of the data gave measurements of the height or wavelength (or both) of the bedforms.

- In 1,365 cases bedform height was quoted,
- in 2,324 cases the bedform wavelength was quoted,
- in 1,229 cases both height and wavelength were quoted,
- and in 2,460 cases either height or wavelength were quoted.

Data is drawn from both field and laboratory measurements, with 1224 field data and 1874 laboratory data. However, the field data are dominated by 908 measurements of wave ripples at a single site (and hence single grain-size and water depth) reported by Traykovski *et al* (1999). This might bias the data statistically. Both field and lab data are useful, although laboratory measurements using regular waves should be treated with caution, since the characteristics of bedforms appear to be different for regular (monochromatic) and irregular waves. In the field, waves are usually classified as irregular with typically a JONSWAP spectrum in shallow water and a Pierson-Moskowitz spectrum in deep water. However, a long period swell in the absence of a local sea can be close to monochromatic.

Restricting attention only to those cases identified as “ripples”, **1,563** cases quoted either height or wavelength. These latter constitute our main data-set for further analysis, although cases with sheet flow/upper stage plane bed are also useful for indicating the flow conditions for which ripples are washed out.

In this section of the report we describe some but not all of the data sources contained in Table 3. There are also some data sources reviewed which are not yet contained in Table 3. Some of the information is based on the earlier review report by Whitehouse and Chesher (1994) and some from SEDMOC (1999). The data review is presented under three headings of current ripples, wave ripples and wave-plus-current ripples.

4.1 CURRENT RIPPLES

Of the 3,098 data assembled, 552 are for currents acting alone.

Allen (1984) has made an extensive review of the available sedimentological literature on bedform morphology and internal structure arising from steady, unsteady and non-uniform flows in fluvial and marine environments. This greatly extends his earlier study of current ripples (Allen, 1968).

Anderson (1942) carried out field measurements in the Enoree river (USA) to study the vertical concentration distribution. At the point of sample collection the river was about 50 feet wide with almost vertical banks. The sand bed consisted of non-uniform material with a mean size of about 700 μm .

Baas (1993, 1994, 1999) and Baas and de Koning (1995) report measurements of ripple development and equilibrium characteristics in steady and quasi-tidal flow. He undertook laboratory flume tests with 0.095 and 0.238mm sand and examined the way in which the ripples developed in time in height, wavelength and plan form.

Bayazit (1969) studied bedform behaviour in a laboratory flume with mobile beds of sand density and less than sand density sediments in simulated tidal flow.

Coleman and Melville (1992) presented laboratory measurements of bedform evolution and migration.

Culbertson *et al* (1972) performed field measurements were carried out at high discharges in the Rio Grande Conveyance Channel, New Mexico in the period from 1965 to 1969. The channel bed consisted of fine sands with median diameters ranging from 0.150 to 0.350mm and the bed forms varied from dunes to flat bed.

Damgaard *et al* (2003) measured the characteristics of sand bedforms and sediment transport in steady unidirectional flow in an enclosed duct at HR Wallingford. The duct was able to be tilted in both positive (upslope in direction of flow) and negative angles and the way in which the bedforms responded to changes in flow speed and bedslope, as well as the interaction with ripple migration transport and suspended sediment transport were investigated.

Dyer (1980) reported measurements adjacent to Skerries Bank, Start Bay, Devon, UK. The site was characterised by rippled medium sand with fine shell in water depth of 14m. Velocity profiles, television monitoring of the bed layer and suspended sediment pumped samples were obtained. The ripples were about 30mm high and of 0.2m wavelength and there was some evidence for the occurrence of ripple flattening at peak tidal flow.

Guy *et al* (1966) is a comprehensive US study of sandy bedforms and sediment transport for a range of sediment sizes.

Kachel and Sternberg (1971) measured the characteristics and migration rate of ripple bedforms on a sandy seabed site in 31m of water. The seabed comprised well sorted medium sand and the seabed ripples were 10 to 50mm in height and 0.1 to 0.5m in wavelength. The data on bedforms was obtained by stereo photographs and the bottom visibility prevented data being collected for longer than about one hour.

Klaasen *et al* (1986) studied the response and characteristics of bedforms under steady and unsteady unidirectional flow in a laboratory flume.

Laursen (1957) measured sand concentration and flow velocity in a laboratory flume with a length of about 30m, a width of 0.9m and a depth of 0.45m. Two size classes of bed material were used, 0.04mm sand and 0.100mm sand. The water depths were in the range of 0.07 to 0.3 m, the depth-averaged velocities were in the range of 0.4 to 0.7m/s. Measurements of the bedform (dune?) sizes could be obtained in the case of the coarser sand.

McLean (1983) made measurements of ripples, megaripples and dunes in the main entrance channel to Jade Inlet, North Sea. The bed comprised fine and medium sand (with grain sizes over 1mm present) and the water depth was 20m. The near bed hydrodynamics was measured and an echo sounding of the bed along a 6m traverse was completed. The megaripples were 2-4m long and 100 to 200mm high, and the ripples were 0.1 to 0.2m long and 10 to 20mm high. The profiling of the bed appeared to indicate an adjustment of the shape of these ripples through the tide.

Raudkivi (1963, 1966) examined the flow over rippled beds, plus bedform generation in laboratory flume studies. Raudkivi and Witte (1990) studied the generation and coalescence of bedforms.

Soulsby (1990) measured the tidal hydrodynamics and benthic boundary layer in 120m of water in the Celtic Sea. The bed was described as silty sand, rippled. No direct measurements of bed topography were made but the variation in measured values of hydraulic bed roughness was explained in terms of the varying orientation of the flow in the open tidal ellipse relative to the crests of the rippled bed. At times of maximum flow the current was flowing normal to the crests and at times of minimum flow parallel to the crests.

Van Rijn (1993) summarises bedform dimensions in steady flow conditions.

Villaret (1994) studied the development of ripples and made hydraulic roughness measurements for steady and stepped-reversing flow in a laboratory flume. The median grain size of the sand bed was 0.09mm. Six tests investigated growth of ripples from a plain bed, three with current reversal and five with increasing/decreasing discharge. The equilibrium ripple dimensions, averaged from the 14 tabulated test results, were wavelength 0.087m and height 8mm. The ripples formed were 2D, 2.5D and 3D in planform shape in different tests and photographs of the bed are included.

Voogt *et al* (1991) measured fluid velocities, sand concentrations and bedforms within some engineering works associated with dyke closure in a tidal channel of the Eastern Scheldt estuary (NL). The median particle size of the bed material was about 0.250mm and bed form data were analysed to determine the bed roughness for flow speeds of up to 2.2 m/s.

Whitehouse *et al* (1998a, b) presented the results of laboratory experiments, carried out at HR Wallingford (UK), on the development of sand ripples in a simulated (rectilinear) tidal flow. The bed sediment was coarse, well sorted quartz sand with d_{50} 0.510mm. The bed profile was measured every half-hour through 6-half tidal cycles. The ripple height, wavelength, ripple steepness and downstream and upstream facing slope angles were calculated. Photographs of the bed were also taken to allow estimates of ripple plan shape to be made. The results showed reversal of bedform crests taking place

within 1 to 1.5 hours after switching of flow direction. Changes in the measured bedform parameters including reduced ripple height and increased wavelength at peak flow were observed. Data was also collected (Whitehouse *et al* 1998b) for the growth of ripples from a flat bed.

Wilkinson (1986) presented data from the same field site as Dyer (1980) but in 20m of water. The data included examples of ripple profiles measured through the tide and analysis for wavelength, ripple height and skewness of slope. The ripple height was about 20mm and the ripple wavelength varied from 0.13 to 0.30m. The data is also presented in Soulsby *et al* (1983).

4.2 WAVE RIPPLES

Of the 3,098 data assembled, 641 are for waves acting alone.

Davies (1984) made measurements of wave-induced ripples on the seabed at Blackpool Sands, Devon (UK). Two experiments were undertaken, hydrodynamics, sediment and ripple profiles were measured. The median size of bed material was 0.78mm and 0.26mm in the two experiments and the water depth varied from 3.6 to 8.2m.

Mogridge *et al* (1994) brought together published data for wave-generated bedforms from field and laboratory measurements. They produced empirical correlations of bedform length and bedform height in terms of a parameter containing sediment size, fluid viscosity density, sediment density and wave period.

O'Donoghue and Clubb (2001) measured ripple bedform development in a large oscillatory flow tunnel in Aberdeen (UK). The experiments involved a range of sand sizes and sinusoidal and asymmetric flows.

Ribberink and Al-Saleem (1989, 1994) measured flow, sand concentrations and bedform (ripple) characteristics in the large oscillating water tunnel at Delft Hydraulics. Tests were conducted with regular and irregular period waves in low and high wave velocity regimes. The tests included sheet-flow conditions where the bedforms were washed out.

Ribberink and Al-Saleem (1991, 1992a, 1992b) made more sand concentration measurements in the large oscillating wave tunnel in the high and low velocity regime. The ripple dimensions were also measured. These tests examined the situation with regular and irregular period (JONSWAP) asymmetric waves.

Roelvink (1987) reported fluid velocities and sand concentrations measured in breaking and non-breaking waves over a sand bed of about 0.210mm size material in the Deltaflume. Irregular waves were generated (Pierson-Moskowitz spectrum). Bed-form characteristics were determined by analysing recordings of an echo-sounder and by visual observation after emptying the flume after some tests. In the case of non-breaking waves the bed was covered with 3D-ripples with height approximately 20mm and length approximately 1m.

Steetzel (1984) made measurements in the oscillating water tunnel of the Delft Hydraulics Laboratory applying a sinusoidal oscillating motion. The sand bed had median diameter of 0.155mm and the tunnel dimensions were width 0.3m and height 0.6 m. Bedforms created by the flow and sediment transport were measured.

Steetzel (1985) reported on flume experiments carried out at the Delft Hydraulics Laboratory to study the dune erosion process. The flume had a length of 50m, a width of 1.2m and a depth of 1.2m. The bed consisted of fine sand with a d_{50} of 0.100mm. Bedforms were present on the sand bed.

Van Rijn (1988) reported results from the same irregular wave tests as Roelvink (1987). Van Rijn concentrated on measurements over 0.200mm sand performed at various locations outside the breaker zone where the local bed slope was almost zero. Bed-form data were determined by analysing recordings of an echo-sounder and by visual observation after emptying the flume. The variation in bedform dimensions was observed; namely, very small ripples with a height of a few millimetres were present in case of relatively large waves. With relatively small waves large-scale three-dimensional bed forms with a height of 20mm and a length of about 1m were present. On top of the large-scale bed forms were superimposed small-scale two-dimensional ripples with a height of 5mm and a length of 0.1m.

Velden (1986) made measurements in the water tunnel of the Delft Hydraulics Laboratory applying a sinusoidal oscillating motion. The tunnel dimensions were width 0.3m and height 0.6m. Three sizes of sand 0.1mm, 0.2mm, 0.36mm were used for the tests. Bedform dimensions were measured along with hydrodynamic and sediment concentration parameters.

Vellinga (1984) carried out measurements in the Deltaflume of the Delft Hydraulics Laboratory. The flume had a length of 233m, a width of 5m and a depth of 7m. The bed consisted of medium fine sand d_{50} of 0.225mm. The bed porosity was about 0.4. The concentration profiles were measured along with the hydrodynamics and a record of the bedform parameters was taken.

4.3 WAVE-PLUS-CURRENT RIPPLES

Of the 3,098 data assembled, 1,905 are for combined waves and currents.

Amos *et al* (1988) reported observations of ripple formations in 22m of water on the seabed off Sable Island, Nova Scotia. The mean diameter of the bed material was 0.23mm. They used photography of the bed to examine the plan configuration of ripples in the prevailing (generally orthogonal) wave and current field. Six well developed ripple types were observed: wave ripples; wave ripples (transitional) with subordinate current ripples in the troughs; wave and current formed ripples; current ripples (transitional) with subordinate wave ripples in the troughs; and current ripples of straight crested and linguoid form. Wave-current ripples formed under co-linear or opposing wave-current conditions were only briefly observed.

Bosman (1982) made flume measurements at the Delft Hydraulics Laboratory to study the vertical concentration distribution. The flume had a length of about 50m, a width of 1.2m and a depth of 1.2m. The bed consisted of fine sand d_{50} of 0.100mm. Various water depths and bed slopes (1:25, 1:80) were used. In some tests a current opposing or following was superimposed on the waves by re-circulating the water through use of a pump. Irregular waves were generated using four different wave spectra. The bed forms were ripples with heights in the range of 10 to 20mm.

Grasmeijer and Sies (1995) presented results of experiments in a flume of the Delft University of Technology with a depth of 1.0m. Irregular waves were generated to produce a peak frequency of 0.4Hz and a JONSWAP spectrum and a co-linear current

was generated. The sediment ripples formed in the sand bed were measured with a bed profiler and the hydrodynamics and sediment concentrations were measured.

Havinga (1992) measured time-averaged fluid velocities and sand concentrations in irregular non-breaking waves combined with a current. The measurements were performed in a wave-current basin $20 \times 26 \text{ m}^2$. The current was confined in a channel parallel to the wave generator – i.e. wave-current orthogonal angle. The bed of the channel consisted of fine sand d_{50} of 0.100mm and the water depth was approximately 0.4m in all tests. Bed form dimensions were measured by means of a bed profile follower. The dimensions of the bed forms in the wave and in the current direction were recorded.

Hoekstra *et al* (2004) studied the form and migration of bedforms on an intertidal shoal at Teignmouth (UK) as part of the EC COAST3D project. They measured hydrodynamics, waves and currents, and bedform height, wavelength and migration speed in a mixed sandy gravel bed. The median grain size of the upper part of the bed deposits was about 0.250 to 0.300mm. The bedform height was of order 50 to 100mm and the wavelength 0.5 to 1.8m. The data is tabulated for inclusion in the bedform database.

Kroon (1991) and Kroon and Van Rijn (1992) measured fluid velocities and sediment concentrations in the (coastal) swash zone and surf zone near Egmond aan Zee (NL). Ripple dimensions were recorded.

Nap and Van Kampen (1988) measured time-averaged fluid velocities, sand concentrations and bedforms in irregular non-breaking waves combined with opposing and following currents over a sand bed of about 0.100mm grainsize. The measurements were performed in a flume with depth of water about 0.5m. The depth-averaged velocities were in the range of 0.1 to 0.4m/s and the significant wave heights were in the range of 0.075 to 0.18m.

Nieuwjaar and van der Kaay (1987) measured time-averaged fluid velocities, sand concentrations and bedforms in irregular non-breaking waves combined with opposing and following currents over a sand bed of about 0.200mm grainsize. The measurements were performed in a flume with depth of water about 0.5m. The depth-averaged velocities were in the range of 0.1 to 0.4m/s and the significant wave heights were in the range of 0.075 to 0.175m.

Lee-Young and Sleath (1990) report laboratory experiments on wave generated ripples plus orthogonal current. They used an oscillating sediment tray and sinusoidal motion. With a weak current the ripples were not significantly different from those induced by pure wave action. They observed that already existing wave vortex generated ripples with straight crests exposed to a current flowing parallel to the crests changed to a serpentine crest planshape.

Ribberink (1995) measured sediment transport in waves and currents in the large oscillating water tunnel at Delft Hydraulics.

Traykovski *et al* (1999) measured bedform dimensions and behaviour off New Jersey in 11m of water over a six-week period with a rotary sidescan sonar system. The influence of time varying waves and currents was monitored. Ripple heights of up to 150mm in height and 0.1m in wavelength were recorded in sand with median grain size of 0.4mm.

Van Rijn *et al* (2002) reported measurements of bedforms on the shoreface at Egmond aan Zee (NL) obtained during the EC COAST3D project. The bedforms vary in type and dimension on the shoreface in response to changes in wave and current action, and grain size. Thorne and Bell (2002) show details of the acoustically measured sand ripple profile on the seabed and how this varies with time.

Vessem (no date) made field measurements near the Galgeplaat, a tidal flat in the Eastern Scheldt estuary in the Netherlands. The measurements of hydrodynamics and sediment concentrations were performed during current and wave conditions from a fixed sampling station. The local sand bed consisted of relatively fine material with a median size of about 0.150mm. The local water depth varied in the range of 0.5 to 4m. and the velocities were not larger than about 1 m/s. The maximum significant wave height was about 0.7m. The reported bed form height was an estimate based on the analysis of velocity profiles resulting in an effective roughness and based on visual inspection of the relict bed forms during the ebb period when the flat was dry.

5. *New predictor for ONR applications (Mark 1)*

5.1 AIMS OF PREDICTOR

The aim is to derive a method of predicting the key ripple descriptors listed in Section 2 (height, spacing, orientation, shape/slope) in terms of input variables of water depth (and temperature and salinity), current speed, wave properties, and sediment properties. These will be combined to give a contour plot and cross-sections of the bed elevation over a local area (say a few metres square).

5.2 EXISTING PREDICTORS

A number of predictors exist for predicting ripple properties. These almost exclusively concentrate on the height and wavelength of the ripples, for either current-generated, wave-generated, or combined flow ripples. The orientation, shape and slope of ripples are much more rarely considered.

Current ripple heights and wavelengths are usually expressed as functions of the grain-diameter (which serves as the length-scale), modulated by the strength of the flow expressed non-dimensionally (such as a Shields parameter or ratio of shear-stress to threshold shear-stress). Van Rijn (1993) and Soulsby (1997) summarise several versions.

Wave ripple heights and wavelengths are usually expressed as functions of the wave orbital diameter (which serves as the length-scale), modulated by a measure of the grain-diameter. The Wiberg and Harris (1994) method combines both orbital diameter and grain-diameter, and is widely used in Europe as well as the USA. It has also been adapted for use in waves-plus-currents (Davies and Villaret, 2000), and cast in a non-iterative form (Malarkey and Davies, 2002).

Comparisons of predictors with data (or with each other) have been made recently by Green (1999), Harris (2004, EstProc project), using the lab data of Thorne *et al* (2002), Foti and Faraci (SANDPIT project, unpublished), and Grasmeijer and Kleinhans (2004). As to the results, Harris favoured the Nielsen (1981) and Wiberg and Harris (1994) methods, Foti and Faraci favoured the (modified) Wiberg and Harris (1994) method, whereas Grasmeijer and Kleinhans found no clear winner out of the Grant and Madsen

(1982), the Van Rijn (1993) and the Nielsen (1981) predictors. Grasmeijer and Kleinhans (2004) proposed their own predictors scaled by wave orbital diameter, and modulated by the wave mobility parameter.

5.3 ANALYSIS AND INTERPRETATION OF DATA-SET

The data-set described in Section 4 has been analysed to derive information about ripple heights and wavelengths. In most cases this has been done separately for ripples generated by currents only, waves only, and combined waves and currents (W+C). We make the assumption that the data-set is a representative, unbiased (but recall the dominance of Traykovski's data) sample of all possible data, and we draw no distinction between field and lab data.

The frequency of occurrence of bedforms of different heights and wavelengths has been derived for a number of categories. Plots of the frequency of occurrence of all the ripple heights in the data-set are shown in Figure 3, divided into bands of 5mm. It is seen that the ripple heights occur most frequently for heights between 10 and 25mm, and reduce in frequency gradually to a height of about 150mm. The few cases with larger heights correspond to dunes in rivers, which are not of interest for the present study.

Likewise Figure 4 shows the frequency of all the wavelengths in bands of 50mm, but restricted to wavelengths less than 4m to exclude river dunes. It is seen that the ripples have two peaks of frequency, one at about 0.10 to 0.15m and one at about 0.7m. The second peak largely corresponds to Traykovski's large data-set. The frequency tails off at about 1.5m, beyond which there is a scattering of long wavelengths.

Figure 5 (which includes only data up to 150mm height) shows the frequencies of ripple heights sub-divided into the different types of forcing. It is seen that current ripples occur most frequently at heights of 25 to 30mm, and wave ripples occur most frequently at 10 to 20mm, while W+C ripples also have a broad peak between about 10 and 20mm. All three tail off at above 60mm, although all have a few cases with heights up to 150mm.

Figure 6 shows a similar subdivided frequency distribution for wavelengths. The current-generated ripples show a single broad peak between about 0.1 and 0.3m, but the wave-generated ripples show one distinct peak centred on about 0.10m. The W+C distribution has three distinct peaks, one centred on about 0.10m and the other on about 0.7m, with a valley between them at about 0.4m, then a third at about 1m.

Dividing the height data into lab and field sources, Figure 7 shows that the shapes of the frequency distributions are similar for lab and field. However, when the wavelength data is similarly divided (Figure 8), it is seen that the long wavelength peak is almost entirely comprised of field data, and further analysis shows that it is predominantly made up from the 908 data of Traykovski *et al* (1999).

The data were further analysed to derive the median (50-percentile), 10-percentile and 90-percentile values of ripple height and wavelength. In this sense, the 90-percentile represents the height which 90% of the data are smaller than (analogous to grain-size, not wave-height). Only data with wavelength smaller than 1.5m were taken, since these are most relevant to the present project. The value 1.5m can be seen in Figure 4 to divide the main distribution from the very sparse tail.

Table 1 shows these percentiles subdivided into waves, currents and W+C, and also subdivided by grain-size. The grain-size bands correspond to the geological phi-scale: $d_{50} = 0.062 - 0.125\text{mm}$, $0.125 - 0.25\text{mm}$, $0.25 - 0.5\text{mm}$, and $0.5 - 1.0\text{mm}$. There were too few cases with $d_{50} > 1\text{mm}$ to include in the analysis. The 10, 50 and 90th percentiles for “all sizes” provided the values quoted in Section 2 for typical ripple heights and wavelengths.

5.4 RIPPLE HEIGHT

The 50th and 90th percentiles for ripple height are plotted against the d_{50} grain-size in Figures 9, 10 and 11 for ripples generated by currents, waves and W+C respectively. The height of ripples is generally believed to (a) increase with grain-size, (b) decrease to zero for grains larger than about $0.8 - 1\text{mm}$. The increase of height with d_{50} is evident for the 50th and 90th percentiles, but only the current-generated ripples potentially show a decrease of height as $d_{50} = 0.8\text{mm}$ is approached.

A formula of the following general form exhibits both of properties (a) and (b):

$$\Delta_n = a.d_{50}.exp(-b.D_*^2) \quad (5.1)$$

where Δ_n is the ripple height at the n 'th percentile, and a and b are coefficients that can be calibrated against the observed data. Values of a and b fitted by eye to the data are shown for each of current, wave and W+C ripples in Table 5. We can consider that the 90th percentile is representative of the largest value that ripple heights can reach (for that grain-size), irrespective of the wave and current flow conditions. The 50th percentile is representative of *all* the ripples (for that grain-size), many of which will have a height less than the maximum because of the flow conditions (e.g. approaching wash-out) or because they are not fully developed (insufficient sediment supply, tidal flows, or lab tests with short run-times).

The values of a in the upper part of Table 5 are in the range 78 to 115 for the 50th percentile (depending on C, W or W+C), telling us that median ripple heights are $78 - 140d_{50}$ for small grain-sizes. The 90th percentiles are roughly twice as large. The values of b are in the range 0.001 to 0.005, which determine the roll-off towards large grain-sizes.

A second term will be included subsequently in Eq (5.1) to account for variations with current speed and wave properties.

5.5 RIPPLE SPACING

A similar approach has been adopted for the wavelengths (see Figures 12, 13, 14 and Table 5). Although the wavelength of ripples is not usually thought to decrease for large grain-sizes in the way that height does, there is some evidence in the data that this is so. Accordingly, a formula of similar form to Eq. (5.1) has been used for the wavelength λ_n at the n 'th percentile:

$$\lambda_n = a.d_{50}.exp(-b.D_*^2) \quad (5.2)$$

The values of a (lower part of Table 5) for current-only and wave-only are typically 10 - 15 times those for heights, implying that typical ripple steepnesses are in the range 1:10 to 1:15. However, W+C values correspond to steeper ripples at about 1:7. The values of b are broadly similar to those for ripple height.

The value of $a = 1000$ obtained for the median wavelength of current-generated ripples corresponds to the commonly-used relation: wavelength = 1000 grain diameters. The 90-percentile value of 1500 also lies within commonly used limits.

A second term will be included subsequently in Eq (5.2) to account for variations with current speed and wave properties.

5.6 RIPPLE ORIENTATION

On the basis of general observations, the azimuth of the crest-line of ripples is perpendicular to the current direction for current ripples, and to the wave propagation direction for wave ripples. For W+C, the ripples are a mixture of those for the current and those for the wave. If either the current or the wave is strongly dominant, the ripple azimuth will follow that one. However, if the current and wave have roughly similar effects the ripple pattern will be complex with no preferred direction.

5.7 RIPPLE SHAPE

We have not yet made a detailed analysis of ripple shape, and there is much less data available to do this. On the basis of general observations, the following shapes are proposed.

Wave ripples make a good starting point, since they are symmetrical and (largely) two-dimensional. Sleath (1984, p 132) proposed a formula to describe the shape of wave ripples mathematically, in such a way that the oscillatory flows above them could be derived analytically.

This formula gives sharp ripple crests and flatter troughs. However, he also says that this shape is observed for fine sediments, but a simple sinusoidal shape is observed for coarse sediments. We here propose a modified version of Sleath's formula, adapted (a) to make it explicit (Sleath's formula is implicit), and (b) to introduce an adjustable "sharpness" parameter ε . Considering a cross-section through the ripple aligned with the wave propagation direction, and calling this direction x , the bed elevation profile $\eta(x)$ is given by:

$$\eta(x) = \frac{\Delta}{2} [\cos(k\xi) + 1] \quad (5.3)$$

$$\text{where } \xi = x + \varepsilon \frac{\Delta}{2} \sin(kx) \quad (5.4)$$

and $k = 2\pi/\lambda$. Here Δ and λ are the height and wavelength of the wave ripple respectively, and η is measured as height above trough level. If $\varepsilon = 0$, then Eq (5.3) is sinusoidal, whereas if ε takes values between 0 and 1, the ripple crests become progressively more peaked. If $\varepsilon = 1$, Eq (5.3) is similar to Sleath's formula, except that Eq (5.4) contains $\sin(kx)$ whereas Sleath has $\sin(k\xi)$. Examples of the shape of this cross-section are shown in Figures 15 and 16.

A similar approach has been taken to define a mathematical shape for current ripples. However, it is more complicated due to the asymmetric, 3D nature of current ripples, and it is not presented in this interim report.

The shape of W+C ripples is assumed to be a mixture of the wave and current shapes, taking account of the fact that waves and currents will generally be in different directions. The best method of combining the wave and current ripple-shape formulae will be determined subsequently.

5.8 CONTOUR PLOTS

Mathematical expressions for the height, wavelength, crest-length, orientation and shape of ripples can be combined to give a mathematical function $\eta(E, N)$ describing the variations in bed elevation over an area of a few square metres as a function of distance East (E) and North (N) of an arbitrary origin.

This is illustrated here for the case of wave-generated ripples. Input parameters are:

- Position in grid coordinates (E, N)
- Direction waves come from, ψ_w , in degrees clockwise of North (compass convention)
- Height of ripples, Δ
- Wavelength of ripples, λ
- “Sharpness” factor, ε .

Values of Δ , λ and ε can be derived (ultimately) from inputs of water depth, current speed, wave height and period, and sediment grain size and density, as described in Sections 5.2 to 5.5. However, for illustrative purposes Δ , λ and ε will be treated as the input parameters. First, convert the coordinates (E, N) to the x-coordinate directed along the wave propagation direction:

$$x = E \cdot \sin \psi_w - N \cdot \cos \psi_w \quad (5.5)$$

Calculate $k = 2\pi/\lambda$, and ξ from Eq (5.4). Then use Eq (5.3) to calculate the value of bed elevation at position (E, N):

$$\eta(E, N) = \frac{\Delta}{2} [\cos(k\xi) + 1] \quad (5.6)$$

A crude mock-up of this procedure has been programmed as an Excel spreadsheet, to show:

- Colour-coded contour plot of bed elevation
- Cross-section North-South through the bed
- Cross-section West-East through the bed.

Examples of the results are shown in Figures 15 and 16, for two values of the inputs.

6. *Tests against existing data*

To be completed before mid-April 2005.

7. *Tests against SAX 99 data*

To be completed on receipt of SAX 99 data.

8. *Proposed work in Phase 2*

The following will be undertaken before the workshop in Seattle May 4-5, 2005.

1. Add any outstanding data to the data-set.
2. Refine analysis of data-set to obtain predictors for ripple height and wavelength in terms of current speed, wave orbital velocity and period, and sediment grain-size and density.
3. Test height and wavelength predictors against the assembled data-set.
4. Obtain data from SAX 99 and test height and wavelength predictors.
5. Complete derivation of contours of bed elevation for current ripples, and for wave-plus-current ripples.
6. Update report to include all the above.

In Phase 2, during and following the Seattle workshop, the following work will be undertaken:

1. Make contact with other Ripples DRI researchers in USA, principally Patricia Wiberg, Peter Traykovski, and Douglas Wilson.
2. Obtain data from SAX 04, and test predictors.
3. Adapt the Mark 1 predictor to include time-history effects, fine sediment effects, slope effects (on larger bedforms), and biological effects.
4. *Either* produce a more sophisticated software package for simulating bed elevation contours, *or* collaborate with Douglas Wilson to build our methods into his existing package.
5. Produce final report.

The Excel spreadsheet showing contours of bed elevation was produced very quickly as a confidence check on the contour-predictor. The intention was to produce a more refined graphical presentation (e.g. using a GIS software tool) in Phase 2. However, at a late stage we became aware of the already-developed graphical user interface described by Wilson (2002). As his work was apparently funded by ONR we will explore the possibilities of collaboration, since it would be more efficient to make use of his graphical interface than to develop a new one.

9. *Conclusions*

In this first phase of the project the following goals have been achieved:

- Discussions have been held with a number of European researchers concerning their work on sea-bed ripples.
- A digest of (some of) the European source publications has been made.
- Data-sets on ripples have been collected, including two large ones in the context of European collaborative projects, and assembled into one large data-set (3,098 entries) in a common format.

- A statistical analysis of this data has been performed to produce frequency distributions of the ripple heights and wavelengths, sub-divided into current-generated (C), wave-generated (W), and wave-plus-current generated (W+C) ripples, and also into lab and field data.
- Percentiles of exceedance of ripple heights and wavelengths, sub-divided into W, C and W+C categories, and also into grain-size categories, have been derived from the data.
- A formula for the dependence of ripple height and wavelength on grain-size has been proposed, and coefficients fitted from the above percentiles analysis. A similar analysis of dependence on flow properties will follow.
- A formula for the shape of wave-ripples has been proposed. A similar formula for current ripples will follow.
- The ingredients of ripple height, wavelength, shape and orientation have been combined into a general formula for the bed elevation as a function of geographical grid coordinates.
- A (crude) graphical display of colour-coded bed elevation and bed cross-sections has been developed, which gives an instant impression of the bed.

The work has concentrated primarily on European data and thinking, since the American partners in the project will already be familiar with American work, and an important reason for our participation is to bring the European work to the project. We will seek to make closer links with US researchers at the Seattle workshop in May 2005.

10. *References and Bibliography*

- Allen, J.R.L., (1968). Current ripples. Amsterdam, North Holland Publishing Company.
- Allen, J.R.L., (1984). Sedimentary Structures: Their Character and Physical Basis, Developments in Sedimentology, vol. 30 (unabridged one-volume edition of the original 1982 2-volume work).
- Allen, J.R.L. and Friend, P.F., (1976). Relaxation time of dunes in decelerating aqueous flows. *J. Geol. Soc. London* 132, 17-26.
- Allen, J.R.L. and Leeder, M.R., (1980). Criteria for the instability of upper-stage plane beds. *Sedimentology* 27, 209-217.
- Allen, J.R.L., (1976). Computational models for dune time-lag: general ideas, difficulties, and early results. *Sedimentary Geology* 15, 1-53.
- Amos, C.L., Bowen, A.J., Huntley, D.A. and Lewis, C.F.M., (1988). Ripple generation under the combined influences of waves and currents on the Canadian continental shelf. *Continental Shelf Research* 8 (10), 1129-1153.
- Amos, C.L., Li, M.Z. and Choung, K.-S., (1996). Storm-generated, hummocky cross-stratification on the outer-Scotian shelf. *Geo-Marine Letters* 16, 85-94.
- Anderson, A.A., (1942). Distribution of Suspended Sediment in a Natural Stream, *Transactions American Geophysical Union, USA*
- Ardhuin, F., Drake, T.G. and Herbers, T.H.C., (2002). Observations of wave-generated vortex ripples on the North Carolina continental shelf. *J. Geophysical Research* 107 (C10), 3143, doi:10.1029/2001JC000986.
- Arnott, R.W. and Southard, J.B., (1990). Exploratory flow-duct experiments on combined-flow bed configurations, and some implications for interpreting storm-event stratification. *Journal of Sedimentary Petrology* 60, 211-219.
- Ashley, G.M., (1990). Classification of large-scale subaqueous bedforms: a new look at an old problem. *J. of Sedimentary Petrology* 60(1), 160-172.
- Baas, J.H., (1993). Dimensional analysis of current ripples in recent and ancient depositional environments. PhD Thesis, University of Utrecht, The Netherlands, 199pp.
- Baas, J.H., (1994). A flume study of the development and equilibrium morphology of current ripples in very fine sand. *Sedimentology* 41, 185-209.
- Baas, J.H., (1999). An empirical model for the development and equilibrium morphology of current ripples in fine sand. *Sedimentology* 46, 123-138.
- Baas, J.H. and de Koning, H., (1995). Washed-out ripples: their equilibrium dimensions, migration rate, and relation to suspended-sediment concentration in very fine sand. *J. of Sedimentary Research* A65(2), 431-435.

- Barton, J.R. and Lin, P.N., (1955). A study of the sediment transport in alluvial channels, Civil Engineering Department, Report No. 55JRBZ, Colorado College, Fort Collins, USA.
- Bayazit, M. (1969). Resistance to reversing flows over movable beds. *Journal of the Hydraulics Division, ASCE*, vol. 95, No. HY4, 1109-1127.
- Bosman, J., (1982). Concentration Distribution under Waves and Current (in Dutch) Report M1875, Delft Hydraulics Laboratory, Delft, The Netherlands.
- Boyd, R., Forbes, D.L., Heffler, D.E., 1988. Time-sequence observations of wave-formed sand ripples on an ocean foreshore. *Sedimentology* 35, 449-464
- Bridge, J.S., (1981). Bed shear stress over subaqueous dunes, and the transition to upper-stage plane beds. *Sedimentology* 28, 33-36.
- Buffington, J.M. and Montgomery, D.R., (1997). A systematic analysis of eight decades of incipient motion studies, with special reference to gravel-bedded rivers. *Water Resources Research* 33 (8), 1993-2029.
- Buffington, J.M. and Montgomery, D.R., (1998). Correction to "A systematic analysis of eight decades of incipient motion studies, with special reference to gravel-bedded rivers". *Water Resources Research* 34 (1), 157.
- Carling, P.A., (1999). Subaqueous gravel dunes. *Journal of Sedimentary Research* 69, 534-545.
- Coleman, S.E. and Melville, B.W., (1992). Bed-form development. *Journal of Hydraulic Engineering*, vol. 120, no. 4, 544-560.
- Culbertson, J.K., Scott, C.H. and Bennet, J.P., (1972). Summary of Alluvial Channel Data from Rio Grande Conveyance Channel, New Mexico 1985-1969. Geological Survey Professional Paper 562-J, Washington, USA.
- Damgaard, J.S., Soulsby, R.L., Peet, A. and Wright, S., (2003). Sand transport on steeply sloping plane and rippled beds. *J. Hyd. Eng., ASCE*, Vol.129, 706-719.
- Davies, A.G., (1984). Field observations of wave-induced motion above the seabed and of the resulting sediment movement. Report No 179, Institute of Oceanographic Sciences, Taunton (UK).
- Davies, A.G. and Villaret, C., (2000). Sand transport by waves and currents: prediction of research and engineering models. ICCE, Sydney, ASCE, 2481-2494.
- Davies, T.R.H., (1982). Discussion of Bridge 1981 (and reply by Bridge). *Sedimentology* 29, 743-747.
- Detle, H. and Uliczka, K., (1986a). Sediment Concentration at Prototype Equilibrium Profile. Technical Report No. 4 - SFB 205/TP A6, University of Hannover, 1986.
- Detle, H. and Uliczka, K., (1986b). Velocity and sediment concentration fields across surf zones. Twentieth Coastal Eng. Conf., Taiwan.

- Dinehart, R.L., (1989). Dune migration in a steep, coarse-bedded stream. *Water Resources Research*, 25(5), pp.911-923.
- Dinehart, R.L., (1992). Evolution of coarse gravel bed forms: field measurements at flood stage. *Water Resources Research* 28, 2667-2689.
- Doucette, J.S., (2000). The distribution of nearshore bedforms and effects of sand suspension on low energy, micro-tidal beaches in Southwestern Australia. *Marine Geology* 165, 41-61.
- Dyer, K.R., (1980). Velocity Profiles Over a Rippled Bed and the Threshold of Movement of Sand. *Estuarine and Coastal Marine Science*, vol 10, pp181-199.
- Dyer, K.R., (1986). *Coastal and Estuarine Sediment Dynamics*. Wiley & Sons, Chichester, UK.
- Forbes, D.L. and Boyd, R., (1987). Gravel ripples on the inner Scotian shelf. *J. of Sedimentary Petrology* 57(1), 46-54.
- Fredsøe, J. and Deigaard, R., (1992). *Mechanics of Coastal Sediment Transport*. World Scientific Publishing.
- Gabel, S.L., (1993). Geometry and kinematics of dunes during steady and unsteady flows in Calamus River, Nebraska, USA. *Sedimentology*, 40, pp.237-269.
- Grant, W.D. and Madsen, O.S., (1982). Movable bed roughness in unsteady oscillatory flow. *J. of Geophysical Research* 87(C1), 469-481.
- Grasmeijer, B. and Sies, R., (1995). Sediment concentrations and sediment transport in irregular breaking waves. Experimental results series A and B. Delft University of Technology, The Netherlands.
- Grasmeijer, B., (2002). Process-based cross-shore modelling of barred beaches, Netherlands Geographical Studies 302, Utrecht, The Netherlands, pp. 251.
- Grasmeijer, B.T., (1995). Sediment concentrations and sediment transport in irregular breaking waves, Experimental Results series A and B, Delft University of Technology, Delft, The Netherlands.
- Grasmeijer, B.T., Kleinhans, M.G., (2004). Observed and predicted bed forms and their effect on suspended sand concentrations, *Coastal Engineering* 51, 351-371.
- Green, M.O., (1999). Test of sediment initial-motion theories using irregular-wave field data. *Sedimentology* 46, 427-441.
- Guy, H.P., Simons, D.B., and Richardson, E.V., (1966). Summary of alluvial channel data from flume experiments 1959-61, US Geological Survey Professional Paper 462-1.
- Hanes, D.M., Alymov, V., Chang, Y.S., (2001). Wave-formed ripples at Duck, North Carolina. *Journal of Geophysical Research* 106 (C10), 22575-22592.

Harris, J.M., (2004). Modelling moveable seabed roughness under random waves. ABPmer Report R. 1092, Southampton, UK, produced for the EstProc project funded by Defra (UK).

Havinga, F.J., (1992). Sediment Concentrations and Sediment Transport in case of Irregular Non-Breaking Waves with a Current. Dept. of Coastal Engng., Delft University of Technology, Delft, The Netherlands.

Hoekstra, P., Bell, P., van Santen, P., Roode, N., Levoy, F. and Whitehouse, R., (2004). Bedform migration and bedload transport on an intertidal shoal. Continental Shelf Research, 24 (11), 1249-1269.

Julien, P.Y. and Raslan, Y., (1998). Upper-regime plane bed. J. of Hydraulic Engineering 124(11), 1086-1096.

Kachel, N. and Sternberg, R.W., (1971). Transport of bedload as ripples during an ebb tidal current. Marine Geology, vol. 10, 229-244.

Klaassen, G.J., Ogink, H.J.M. and van Rijn, L.C., (1986). DHL - research on bedforms, resistance to flow and sediment transport. Presented at 3rd International Symposium on River Sedimentation, Jackson (MS), U.S.A., March 31 - April 4, 1986. Delft Hydraulics Communication No 362.

Kleinhans, M.G., Wilbers, A.W.E., De Swaaf, A. and Van den Berg, J.H., (2002). Sediment supply-limited bedforms in sand-gravel bed rivers. J. of Sedimentary Research 72(5), 629-640.

Kleinhans, M.G., (2005). Phase diagram of bed states insteedy, unsteady, oscillatory and mixed flows. Paper Q of SANDPIT Book to be published July 2005.

Komar, P.D. and Miller, M.C., (1975). The initiation of oscillatory ripple marks and the development of plane-bed at high shear stresses under waves. J. of Sedimentary Petrology 45(3), 697-703.

Kroon, A., (1991). Suspended sediment concentrations in a barred nearshore zone, Coastal Sediments, Seattle, USA.

Kroon, A., and van Rijn, L.C., (1992). Suspended sediment fluxes in the nearshore zone at Egmond, Department of Physical Geography, University of Utrecht, The Netherlands.

Lauchlan, C.S., (2004). Experimental investigation of bed-load and suspended-load transport over weirs, Journal of Hydraulic Research, Vol. 42, No.5, pp549-555.

Laursen, E.M., (1957). An investigation of the total sediment load, IOWA Institute of Hydraulic Research, State University of Iowa, Iowa City, USA.

Lee Young, J.S. and Sleath, J.F.A., (1990). Ripple formation in combined transdirectional steady and oscillatory flow. Sedimentology, 37, 509-516.

- Li, M.Z. and Amos, C.L., (1998). Predicting ripple geometry and bed roughness under combined waves and currents in a continental shelf environment. *Continental Shelf Research* 18: 941-970.
- Li, M.Z. and Amos, C.L., (1999a). Sheet flow and large wave ripples under combined waves and currents: field observations, model predictions and effects on boundary layer dynamics. *Continental Shelf Research* 19, 637-663.
- Li, M.Z. and Amos, C.L., (1998). Predicting ripple geometry and bed roughness under combined waves and currents in a continental shelf environment. *Continental Shelf Research* 18: 941-970.
- Li, M.Z., Wright, L.D., and Amos, C.L., (1996). Predicting ripple roughness and sand resuspension under combined flows in a shoreface environment. *Marine Geology* 130: 139-161.
- Lofquist, K.E.B., (1978). Sand ripple growth in an oscillatory flow water tunnel, US Army Corps of Engineers, Coastal Engineering Research Centre, Technical Paper No. 78-5.
- Malarkey, J. and Davies, A.G., (2002). A non-iterative procedure for the Wiberg and Harris (1994) oscillatory sand ripple predictor. Accepted for publication in *J. Coast. Res.*
- McLean, S.R., (1983). Turbulence and Sediment Transport Measurements in a North Sea Tidal Inlet (The Jade). In: *North Sea Dynamics*. Eds. J. Si ndermann and W Lenz, Pub. Springer-Verlag Berlin, Heidelberg, pp436-452.
- Mogridge, G.R., Davies, M.H. and Willis, D.H., (1994). Geometry prediction for wave-generated bedforms. *Coastal Engineering*, 22, 255-286.
- Myrow, P.M. and Southard, J.B., (1991). Combined-flow model for vertical stratification sequences in shallow marine storm-deposited beds. *J. of Sedimentary Research* 61 (2), 202-210.
- Nap, E.N. and Van Kampen, H.F.A., (1988). Sediment Concentrations and Sediment Transport in case of Irregular Non-Breaking Waves with a Current. Delft University, Coastal Engineering Department, Delft, The Netherlands.
- Nielsen, P., (1981). Dynamics and geometry of wave-generated ripples. *J. of Geophysical Research* 86(C7), 6467-6472.
- Nielsen, P., (1984). Field Measurements of Time-Averaged Suspended sediment concentrations under waves, *Coastal Engineering* 8, 51-72.
- Nielsen, P., (1992). Coastal bottom boundary layers and sediment transport. *Advanced Series on Ocean Engineering* 4, World Scientific, Singapore, 324.
- Nieuwjaar, M. and Kaay, Th. van der, (1987). Sediment Concentrations and Sediment Transport in case of Irregular Non-Breaking Waves with a Current. Delft University, Civil Engineering, Delft, The Netherlands [there is also a journal paper].

O'Donoghue, T. and Clubb, G.S., (2001). Sand ripples generated by regular oscillatory flow. *Coastal Eng.*, 44, pp. 101-115.

O'Donoghue, T., Doucette, J.S., van der Weerf, J.J. and Ribberink, J.S., (2005). Flow tunnel measurements of full-scale ripples in oscillatory flow. Paper V of SANDPIT Book to be published July 2005.

Parker, G. in prep. Transport of gravel and sediment mixtures. In: ASCE Manual 54, Sedimentation Engineering, Garcia, M. in prep. (ed.), draft on <http://www.ce.umn.edu/~parker/>.

Raudkivi, A.J., (1963). Study of sediment ripple formation. *Journal of the Hydraulics Division, ASCE*, vol. 89, no. HY6, 15-33.

Raudkivi, A.J. (1966). Bed forms in alluvial channels. *Journal of Fluid Mechanics*, 26, 507-514.

Raudkivi, A.J. and Witte, H-H., (1990). Development of bed features. *Journal of Hydraulic Engineering, ASCE*, vol. 116, no. 9, 1063-1078.

Ribberink, J.S., (1995). Time-averaged sediment transport phenomena in combined wave-current flows. Part II, Report H1889.11, Delft Hydraulics, Delft, The Netherlands.

Ribberink, J.S. and Al-Salem, A.A., (1989). Bed forms, near bed sediment concentrations and sediment transport in simulated regular wave conditions, Report H840, Part III, Delft Hydraulics, Delft, The Netherlands.

Ribberink, J.S. and Al-Salem, A., (1991). Sediment Transport, Sediment Concentrations and Bed Forms in Simulated Asymmetric Wave Conditions. Report H840.20 Part IV, Delft Hydraulics, The Netherlands.

Ribberink, J.S. and Al-Salem, A., (1992a). Sediment Transport, Sediment Concentrations and Bed Forms in Simulated Asymmetric Wave Conditions. Report H840.20 Part V, Delft Hydraulics, Delft, The Netherlands.

Ribberink, J.S. and Al-Salem, A., (1992b). Time-Dependent Sediment Transport Phenomena in Oscillatory Boundary Layer Flow under Sheet Flow Conditions. Report H840.20 Part VI, Delft Hydraulics, Delft, The Netherlands.

Ribberink, J.S. and Al-Salem, A.A., (1994). Sediment transport in oscillatory boundary layers in cases of rippled beds and sheet flow. *J. of Geophysical Research* 99(C6), 12707-12727.

Roelvink, J.A., (1987). Large scale investigation of cross-shore sediment transport. Report H596, Delft Hydraulics, Delft, The Netherlands.

Scott, G.H. and Stephens, H.D., (1966). Special Sediment Investigation, Mississippi River at St. Louis, Missouri, 1961-1963 Geol. Survey Water-supply Paper 1819-J, Washington, USA.

SEDMOC, (1999). SEDMOC Database TAP. Instruction Manual. April 1999. Delft Hydraulics/Delft University of Technology. EC MAST project.

- Simons, D.B. and Richardson, E.V., (1965). A study of variables affecting flow characteristics and sediment transport in alluvial channels. In: Federal Inter-Agency Sediment Conference 1963 Proceedings: US Department of Agriculture publication 970, 193-207.
- Sleath, J.F.A., (1984). Sea Bed Mechanics. Wiley, New York.
- Soulsby, R.L., (1987). Calculating bottom orbital velocity beneath waves. Coastal Engineering 11, 371-380.
- Soulsby, R.L., (1990). Tidal-current boundary layers. In: The Sea, vol 9, Part A, Ocean Engineering Science. Eds. B. Le Mehaute and D.M. Hanes, Pub. John Wiley and Sons, New York, pp523-566.
- Soulsby, R.L., (1997). Dynamics of marine sands. Thomas Telford Publications, London, United Kingdom.
- Soulsby, R.L., Davies, A.G. and Wilkinson, R.H., (1983). The detailed processes of sediment transport by tidal currents and by surface waves. Institute of Oceanographic Sciences Report No 152, 80pp.
- Southard, J.B. and Boguchwal, A.L., (1990). Bed configurations in steady unidirectional water flows. Part 2. Synthesis of flume data: Journal of Sedimentary Petrology 60, 658-679.
- Southard, J.B., Lambié, J.M., Federico, D.C., Pile, H.T. and Weidman, C.R., (1990). Experiments on bed configurations in fine sands under bidirectional purely oscillatory flow, and the origin of hummocky cross-stratification. Journal of Sedimentary Petrology 60, 1-17.
- Steezel, H.J., (1984). Sediment suspension in an oscillating water motion close to the sand bed (in Dutch), Coastal Engineering Department, Delft University of Technology, Delft, The Netherlands.
- Steezel, H.J., (1985). Model Tests of Scour near the Toe of Dune Revetments (in Dutch).
- Steezel, H.J., (1987). Systematic investigation of dune revetments: large scale model tests, Report H298-I, Delft Hydraulics, Delft, The Netherlands.
- Sternberg, R.W. and Larsen, L.H., (1975). Threshold of sediment movement by open ocean waves: observations. Deep-Sea Research 22, 299-309.
- Ten Brinke, W.B.M., Gruyters, S.H.L.L., Koomans, R.L., Wilbers, A.W.E. and Kleinhans, M.G., (submitted). Sediment transport and morphological processes near a river bifurcation in the Dutch Rhine, submitted to the Proc. 7th Int. Conf. Fluv. Sed.
- Terwindt, J.H.J. and Brouwer, M.J.N., (1986). The behaviour of intertidal sandwaves during neap-spring tidal cycles and the relevance for palaeoflow reconstruction. Sedimentology, 33, 1-31.

- TNO-NITG, (2000). Descriptions and photographs of the vibrocores in the Niederrhein, Bovenrijn, Waal and Pannerdensch Kanaal. Dutch Institute for Applied Geology (TNO-NITG), The Netherlands.
- Thorne, P.D. and Bell, P.S., (2002). Acoustic measurements of suspended sediments and bedform morphology during the main Egmond experiment. Paper G in Van Rijn *et al* (2002).
- Thorne, P.D., Williams, J.J. and Davies, A.G., (2002). Suspended sediments under waves measured in a large-scale flume facility. J. Geophys. Res., 107, C8.
- Traykovski, P., Hay, A.E., Irish, J.D. and Lynch, J.F., (1999). Geometry, migration, and evolution of wave orbital ripples at LEO-15. Journal of Geophysical Research 104 (C1), 1505-1524.
- Van de Meene, J.W.H., Boersma, J.R. and Terwindt, J.H.J., (1996). Sedimentary structures of combined flow deposits from the shoreface-connected ridges along the central Dutch coast. Marine Geology 131, 151-175.
- Van den Berg, J.H. and Van Gelder, A., (1993). A new bedform stability diagram, with emphasis on the transition of ripples to plane bed in flows over fine sand and silt: Special Publications of the International Association of Sedimentologists 17, 11-21.
- Van Rijn, L.C., (1984). Sediment transport, part I: bed load transport, J.of Hydraul. Eng. 110(10), 1431-1456.
- Van Rijn, L.C., (1988). Handbook of Sediment Transport in currents and waves. Delft Hydraulics, Delft, The Netherlands.
- Van Rijn L.C., (1993). Principles of Sediment Transport in Rivers, Estuaries and Coastal Seas. Aqua Publications, Amsterdam.
- Van Rijn, L.C., Ruessink, B.G. and Mulder, J.P.M., (2002). COAST3D-Egmond. The behaviour of a straight sandy coast on the time scale of storms and seasons. End document. EC MAST project No MAS3-CT97-0086.
- Velden, E. van der, (1986). Sediment Suspension in an oscillating Water Motion close to the Sand Bed (in Dutch). Coastal Engineering Dep, Delft Univ. of Technology, Delft, The Netherlands.
- Vellinga, P., (1984). Large-scale Dune Erosion Tests in the Deltaflume (in Dutch). Report M1263-III A/B, Delft Hydraulics Laboratory, Delft, The Netherlands.
- Vessem, (no date). Rijkswaterstaat, Deltadienst, Den Haag. Project Geomor.
- Villaret, C., (1994). Ripples development and equivalent roughness measurements in unsteady flow conditions. Laboratoire National D'Hydraulique, Chatou, France. Report HE-42/94/16.
- Voogt, L., Van Rijn, L.C. and Van de Berg, J.H., (1991). Bed roughness and transport of fine sands at high velocities. Journal of Hydraulic Engineering, ASCE, HY7.

- Whitehouse, R.J.S. and Chesher, T.J., (1994). Seabed roughness in tidal flows: A review of existing measurements. HR Wallingford Report SR360.
- Whitehouse, R.J.S., Mitchener, H.J. and Soulsby, R.L., (1998a). Ripple characteristics and bed roughness under tidal flow. Proceedings Coastal Dynamics '97, Plymouth, UK, ed. E B Thornton, ASCE, 1043-1052.
- Whitehouse, R.J.S., Mitchener, H.J. and Soulsby, R.L., (1998b). Laboratory experiments on ripple development and bed roughness in tidal flow. Data Report. Report TR66, October 1988, HR Wallingford, UK.
- Wiberg, P.L. and Harris, C.K., (1994). Ripple geometry in wave-dominated environments. J. Geophys. Res., 99 (C1), 775-789.
- Wiberg, P.L. and Smith, J.D., (1987). Calculations of the critical shear stress for motion of uniform and heterogeneous sediments. Water Resources Research 23(8), 1471-1480.
- Wilbers, A., (2004). The development and hydraulic roughness of subaqueous dunes. Netherlands Geographical Studies 323 (PhD-thesis), The Royal Dutch Geographical Society, Faculty of Geosciences, Utrecht University, The Netherlands, 227 pages.
- Wilkinson, R.H., (1986). Variation of roughness length of a mobile sand bed in a tidal flow. Geo-Marine Letters, 5, 231-239.
- Wilson, D.J., (2002). Computer Simulation of Sand Ripple Growth and Migration. Report to US Office of Naval Research Sensing and Systems Division (Code 321), Marine Geosciences: FY02 Annual Reports.
- Wilson, K.C., Andersen, J.S. and Shaw, J.K., (1995). Effects of wave asymmetry on sheet flow. Coastal Engineering 25, 191-204.
- Zanke, U.C.E., (2003). On the influence of turbulence on the initiation of sediment motion, International J. of Sediment Research 18(1), 1-15.

Tables

Table 1 Summary of percentiles of ripple height and wavelength subdivided by grain size

maximum length 1.5m

this is the maximum wavelength considered for ripples

Ripple height (m)

| d ₅₀ size range (mm) | | flow type | number of data | 10-percentile | 50-percentile | 90-percentile |
|---------------------------------|-------|-----------|----------------|---------------|---------------|---------------|
| min | max | | | | | |
| 0.06 | 0.125 | C | 21 | 0.007 | 0.009 | 0.030 |
| | | W | 57 | 0.007 | 0.011 | 0.020 |
| | | W + C | 126 | 0.006 | 0.008 | 0.013 |
| 0.125 | 0.25 | C | 46 | 0.009 | 0.016 | 0.026 |
| | | W | 277 | 0.008 | 0.020 | 0.050 |
| | | W + C | 69 | 0.011 | 0.018 | 0.047 |
| 0.25 | 0.5 | C | 31 | 0.006 | 0.018 | 0.055 |
| | | W | 68 | 0.011 | 0.035 | 0.060 |
| | | W + C | 121 | 0.010 | 0.019 | 0.080 |
| 0.5 | 1 | C | 87 | 0.015 | 0.023 | 0.029 |
| | | W | 1 | 0.060 | 0.060 | 0.060 |
| | | W + C | 89 | 0.019 | 0.040 | 0.099 |
| all | all | C | 197 | 0.008 | 0.021 | 0.033 |
| | | W | 403 | 0.008 | 0.020 | 0.050 |
| | | W + C | 405 | 0.007 | 0.016 | 0.075 |

Ripple length (m)

| d ₅₀ size range (mm) | | flow type | number of data | 10-percentile | 50-percentile | 90-percentile |
|---------------------------------|-------|-----------|----------------|---------------|---------------|---------------|
| min | max | | | | | |
| 0.06 | 0.125 | C | 30 | 0.048 | 0.085 | 0.138 |
| | | W | 124 | 0.055 | 0.110 | 0.207 |
| | | W + C | 132 | 0.046 | 0.064 | 0.102 |
| 0.125 | 0.25 | C | 55 | 0.067 | 0.150 | 0.216 |
| | | W | 287 | 0.070 | 0.165 | 1.000 |
| | | W + C | 135 | 0.070 | 0.130 | 0.692 |
| 0.25 | 0.5 | C | 31 | 0.152 | 0.366 | 1.372 |
| | | W | 78 | 0.077 | 0.200 | 0.443 |
| | | W + C | 1031 | 0.200 | 0.636 | 0.927 |
| 0.5 | 1 | C | 87 | 0.196 | 0.266 | 0.805 |
| | | W | 1 | 0.500 | 0.500 | 0.500 |
| | | W + C | 92 | 0.123 | 0.253 | 0.549 |
| all | all | C | 215 | 0.079 | 0.204 | 0.811 |
| | | W | 490 | 0.068 | 0.150 | 0.550 |
| | | W + C | 1395 | 0.089 | 0.550 | 0.847 |

The totals in “all” include bedform data for grain size ranges <0.06mm and >1.0mm.

Table 2 Tentative bed state definitions proposed by Kleinhans. *Reproduced from Kleinhans (2005) with permission*

| Bed state name | Tentative bed state definition |
|------------------------------|--|
| lower stage plane bed | plane bed with maximum roughness lengths of $O(d_{50})$ for a plot of size $O(1m^2)$ (excluding biogenic features), no or marginal motion of sediment |
| upper stage plane bed | plane bed with maximum roughness lengths of $O(d_{50})$ for a plot of size $O(1m^2)$ with much sediment suspension and a sediment layer of several d_{50} thick in motion by the flow, associated with large orbital and/or current flow velocities but subcritical flow ($Fr < 0.8$), containing parallel lamination |
| upper flow regime, antidunes | plane or undulating bed with undulations moving against the flow direction, associated with critical flow (plane bed, $Fr \sim 0.84$) or supercritical flow ($Fr > 1$) |
| current ripples | linguoid bedforms with maximum length $O(0.4m)$ and height $O(0.02m)$, equilibrium dimensions are independent of flow conditions, non-equilibrium form may be straight-crested, associated with hydraulic smooth flow ($Re^* < 11.6$) or $d_{50} < 0.7$ mm, containing small-scale cross-stratification |
| current dunes | approximately triangular cross-sections but often convex-upwards stoss sides, lee side commonly at angle of repose and vortex shedding, observed height and length from smaller than current ripple sizes to $O(10m)$ high and $O(100m)$ long, equilibrium dimensions depend on flow conditions, e.g. dune height is 0.15-0.35 of water depth, associated with hydraulic rough flow ($Re^* > 11.6$) or $d_{50} > 0.7$ mm, containing large-scale cross-stratification, |
| 3D vs 2D dunes | 2D dunes are straight or wavy-crested with small variations in dune top height and trough scour depth, whereas 3D dunes are lunate, cusped or linguoid with much variation in dune top height and trough scour depth, transition 2D to 3D is associated with sediment mobility or, alternatively, 2D dunes are not in equilibrium with the flow |
| wave ripples | concave-upwards two-sided (or more) slip faces, maybe straight-crested in sand of $d_{50} > 0.5$ mm and calm conditions but otherwise highly irregular, when sharp-crested with top angles approximating the angle of repose, there is also vortex shedding from the tops |
| hummocks | convex-upwards semi-spherical forms in an irregular spatial pattern, observed heights $O(0.1m)$ and lengths $O(1-10m)$, with much sediment suspension but no strong vortex shedding, associated with large orbital flows possibly combined with small currents but origin unclear, containing Hummocky Cross-Stratification (HCS): semi-parallel lamination in undulating bands |
| mixed flow ripples | bedforms with characteristics of both flow and current bedforms, e.g., weak current action on wave bedforms in following or opposing current causes skewness in the current direction, perpendicular small currents and waves give current ripples in the troughs of wave ripples, weak wave action on current bedforms causes rounding, equal current and wave action commonly causes irregular bedforms |
| long wave ripples | wave ripples larger than, and subimposed on commonly found wave ripples while both are active and stable, origin unclear but possibly similar to skewed hummocks |
| megaripples | in currents probably equal to dunes, in waves origin unclear but possibly similar to skewed hummocks |

$$Fr = \text{Froude Number} = \frac{U}{(gh)^{0.5}} \quad \text{with } U \text{ flow velocity, } g \text{ acceleration due to gravity and } h \text{ flow depth}$$

$$Re^* = \text{Grain Reynolds Number} = \frac{u_* d}{\nu} \quad \text{with } u_* \text{ the skin friction shear velocity, } d \text{ the grain diameter and the } \nu \text{ kinematic viscosity of the water}$$

Table 3 Summary of data sources and types of data available

| Source | No of current data | No of wave data | No of W + C data | No of lab data | No of field data | ripple height (m) | | ripple wave length (m) | | average water depth (m) | | d ₅₀ (mm) | |
|--|--------------------|-----------------|------------------|----------------|------------------|-------------------|-------|------------------------|--------|-------------------------|--------|----------------------|-------|
| | | | | | | min | max | min | max | min | max | min | max |
| Baas (1999) | 11 | | | 11 | | | | 0.035 | 0.072 | 0.323 | 0.350 | 0.238 | 0.238 |
| Baas (1994) | 17 | | | 17 | | | | | 0.079 | 0.315 | 0.340 | 0.095 | 0.095 |
| Baas and Koning (1995) | 23 | | | 23 | | | | | | 0.367 | 0.405 | 0.108 | 0.108 |
| Van den Berg and Van Gelder (1993) | 12 | | | 12 | | 0.013 | 0.034 | 0.180 | 0.180 | 0.320 | 0.450 | 0.033 | 0.033 |
| Guy <i>et al</i> (1966) | 90 | | | 90 | | 0.002 | 0.198 | 0.088 | 7.315 | 0.134 | 0.375 | 0.178 | 1.030 |
| Gabel (1993) | 27 | | | 0 | 27 | 0.097 | 0.195 | 2.000 | 4.050 | | | 0.250 | 0.410 |
| Doucette (2000) | | 58 | | 0 | 58 | | 0.110 | | 0.700 | 0.250 | 1.730 | 0.140 | 0.530 |
| O'Donoghue and Clubb (2001) | | 44 | | 44 | | | | | | | | 0.180 | 0.440 |
| O'Donoghue, Doucette, van der Weerf and Ribberink (2005) | | 20 | | 20 | | | | 0.001 | 0.554 | 0.420 | 1.330 | 0.220 | 0.440 |
| Lofquist (1978) | | | 104 | 104 | | 0.016 | 0.155 | 0.110 | 1.685 | | | 0.550 | 0.550 |
| Terwindt and Brouwer (1986), also Ashley (1990) | 53 | | | | 53 | | | | | 0.810 | 3.400 | 0.200 | 0.230 |
| Grasmeijer (2002) | | | 48 | | 48 | | | | | 1.410 | 5.286 | 0.220 | 0.220 |
| Kleinhans (unpublished) | 10 | | | | 10 | 0.087 | 0.499 | 3.220 | 18.861 | 8.600 | 10.686 | 0.564 | 0.945 |
| Dinehart (1989,1992) | 25 | | | | 25 | 0.143 | 0.410 | 6.900 | 34.933 | 1.400 | 2.235 | 0.022 | 0.036 |
| Arnott and Southard (1990) | | | 79 | 79 | | | | | | 0.260 | 0.260 | 0.090 | 0.090 |
| Hanes, Alymov and Chang (2001) | | | 223 | | 223 | | | 0.050 | 0.250 | 1.400 | 7.000 | 0.121 | 1.662 |
| Traykovski, Hay, Irish and Lynch (1999) | | | 908 | | 908 | | | 0.010 | 1.063 | 11.000 | 11.000 | 0.400 | 0.400 |
| Li and Amos (1999b) | | | 11 | | 11 | | | 0.000 | 0.800 | 55.800 | 56.700 | 0.200 | 0.200 |
| Boyd, Forbes and Heffler (1988) | | 68 | | | 68 | | | 0.070 | 0.240 | 9.600 | 12.500 | 0.110 | 0.110 |
| Li and Amos (1998) | | | 35 | | 35 | 0.008 | 0.022 | 0.077 | 0.154 | 38.710 | 40.030 | 0.340 | 0.340 |
| Li and Amos (1999a) | | | 38 | | 38 | 0.009 | 0.060 | 0.070 | 0.600 | 39.000 | 39.000 | 0.340 | 0.340 |
| Ribberink and Al-Salem (1994), Ribberink (1995) | | 45 | | 45 | | 0.003 | 0.350 | 0.080 | 2.700 | | | 0.210 | 0.210 |
| Nielsen (1984) | | | 65 | | 65 | 0.005 | 0.200 | 0.050 | 1.500 | 0.800 | 1.830 | 0.110 | 0.620 |
| Bosman (1982) | | | 64 | 64 | | 0.010 | 0.030 | | | 0.100 | 0.600 | 0.105 | 0.105 |
| Vellinga (1984) | | 11 | | 11 | | | 0.040 | 1.000 | 1.000 | 0.800 | 3.400 | 0.225 | 0.225 |
| Steetzel (1985) | | 7 | | 7 | | 0.020 | 0.020 | 0.080 | 0.080 | 0.260 | 0.650 | 0.095 | 0.095 |
| Anderson (1942) | 23 | | | | 23 | | | | | 0.920 | 1.570 | 0.700 | 0.700 |
| Scott and Stephens (1966) | 23 | | | | 23 | | | | | 4.640 | 16.350 | 0.180 | 0.400 |

Table 3 Summary of data sources and types of data available (continued)

| Source | No of current data | No of wave data | No of W + C data | No of lab data | No of field data | ripple height (m) | | ripple wave length (m) | | average water depth (m) | | d ₅₀ (mm) | |
|---|--------------------|-----------------|------------------|----------------|------------------|-------------------|-------|------------------------|-------|-------------------------|--------|----------------------|-------|
| | | | | | | min | max | min | max | min | max | min | max |
| Barton and Lin (1955) | 26 | | | 26 | | | 0.029 | | 0.230 | 0.110 | 0.420 | 0.180 | 0.180 |
| Vessem (unknown) | | | 70 | | 70 | 0.050 | 0.050 | | | 0.690 | 4.040 | 0.150 | 0.150 |
| Steetzel (1984) | | 105 | | 105 | | 0.005 | 0.100 | 0.030 | 0.550 | 0.400 | 0.400 | 0.220 | 0.220 |
| Velden (1986) | | 154 | | 154 | | 0.005 | 0.080 | 0.011 | 0.450 | 0.400 | 0.400 | 0.100 | 0.360 |
| Roelvink (1987) | | 26 | | 26 | | 0.020 | 0.020 | 1.000 | 1.000 | 0.710 | 2.720 | 0.215 | 0.240 |
| Steetzel (1987) | | 8 | | 8 | | | | | | 0.780 | 1.630 | 0.208 | 0.208 |
| van Rijn (1988) | | 13 | | 13 | | 0.001 | 0.030 | 0.150 | 1.000 | 1.850 | 2.800 | 0.190 | 0.230 |
| Nieuwjaar and Kaay (1987) | | | 28 | 28 | | 0.011 | 0.029 | 0.089 | 0.200 | 0.490 | 0.520 | 0.200 | 0.223 |
| Nap and van Kampen (1988) | | | 30 | 30 | | 0.002 | 0.015 | 0.006 | 0.145 | 0.480 | 0.520 | 0.095 | 0.113 |
| Voogt, van Rijn and van de Berg (1991) | 60 | | | | 60 | | | | | 5.900 | 10.800 | 0.225 | 0.345 |
| Culbertson, Scott and Bennet (1972) | 22 | | | | 22 | | | | | 1.130 | 1.760 | 0.160 | 0.330 |
| Detle and Uliczka (1986a, 1986b) | | 11 | | 11 | | | | | | 0.960 | 2.600 | 0.330 | 0.330 |
| Laursen (1957) | 12 | | | 12 | | 0.019 | 0.033 | 0.116 | 0.146 | 0.080 | 0.300 | 0.040 | 0.100 |
| Ribberink and Al-Salem (1989) | | 48 | | 48 | | 0.016 | 0.350 | 0.137 | 3.000 | 0.800 | 0.800 | 0.210 | 0.210 |
| Havinga (1992) | | | 28 | 28 | | 0.006 | 0.014 | 0.064 | 0.111 | 0.400 | 0.430 | 0.100 | 0.100 |
| Kroon (1991), Kroon and van Rijn (1992) | | | 62 | 0 | 62 | 0.010 | 0.050 | 0.150 | 0.750 | 0.390 | 1.520 | 0.300 | 0.474 |
| Ribberink and Al-Salem (1991, 1992b) | | 23 | | 23 | | 0.003 | 0.014 | 0.084 | 0.110 | 0.800 | 0.800 | 0.210 | 0.210 |
| Grasmeijer (1995) | | | 67 | 67 | | 0.005 | 0.021 | 0.038 | 0.129 | 0.290 | 0.600 | 0.095 | 0.095 |
| Grasmeijer and Kleinhans (2004) | | | 45 | 0 | 45 | 0.007 | 0.100 | 0.190 | 2.000 | 1.410 | 5.290 | 0.240 | 0.240 |
| Lauchlan (2004) | 6 | | | 6 | | 0.011 | 0.015 | 0.095 | 0.207 | 0.260 | 0.410 | 0.164 | 0.164 |
| Damgaard, Soulsby, Peet and Wright (2003) | 22 | | | 22 | | | 0.030 | | 0.220 | 0.200 | 0.200 | 0.231 | 0.237 |
| Villaret (1994) | 14 | | | 14 | | 0.005 | 0.011 | 0.064 | 0.109 | 0.280 | 0.298 | 0.090 | 0.090 |
| Whitehouse <i>et al</i> (1998a, 1998b) | 76 | | | 76 | | 0.002 | 0.032 | 0.099 | 0.489 | 0.194 | 0.250 | 0.510 | 0.510 |
| | 552 | 641 | 1905 | 1224 | 1874 | | | | | | | | |

Table 4 Classification of available data

Total number of data 3098

| Flow type | | Bedform type | | Test conditions | |
|---------------------|------|--------------|------|-----------------|------|
| current only data | 552 | ripples | 1751 | Laboratory | 1224 |
| wave only data | 641 | mega ripples | 19 | Field | 1874 |
| wave + current data | 1905 | dunes | 119 | not given | 0 |
| not defined | 0 | plane bed | 228 | | |
| Total | 3098 | | 2117 | | 3098 |

Table 5 Coefficients a and b in ripple height and wavelength predictors

| Percentile | Current | | Waves | | Waves-plus-current | |
|------------|--------------------|--------|-------|--------|--------------------|--------|
| | a | b | a | b | a | b |
| | Ripple heights | | | | | |
| 50th | 78 | 0.0025 | 115 | 0.001 | 95 | 0.0018 |
| 90th | 225 | 0.0049 | 200 | 0.0025 | 250 | 0.0018 |
| | Ripple wavelengths | | | | | |
| 50th | 1000 | 0.0029 | 1100 | 0.0016 | 2500 | 0.006 |
| 90th | 1500 | 0.001 | 2800 | 0.004 | 3800 | 0.0048 |

Ripple height and length predictor for 50-percentiles and 90-percentiles.

Coefficients in the expression: Δ_n or $\lambda_n = a.d_{50}.\exp(-b.D_*^2)$

Figures

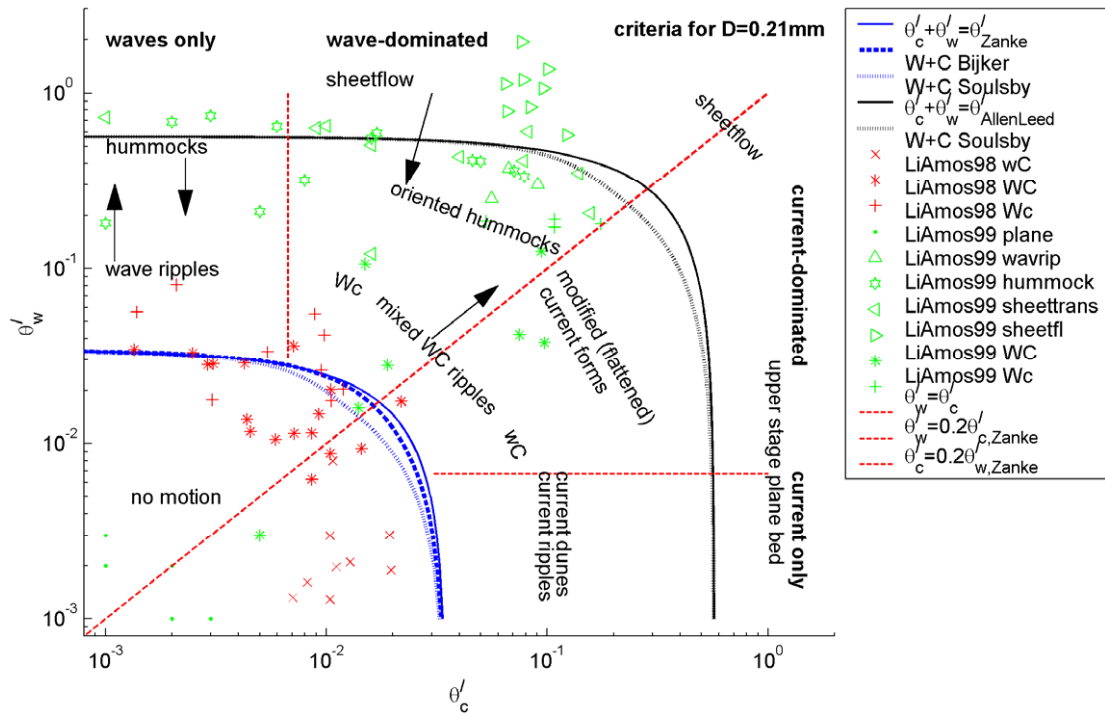


Figure 1 Bedform existence diagram for waves plus currents using Shields' parameters proposed by Kleinhans, based on rational criteria for beginning of motion and sheetflow/USPB (here plotted for $D=0.21$ mm)

Regions of wave or current dominance are indicated by given ratios of wave and current Shields values. Mixed wave-current ripples vary much in morphology depending partly on the angle between currents and waves. *Reproduced from Kleinhans (2005) with permission.*

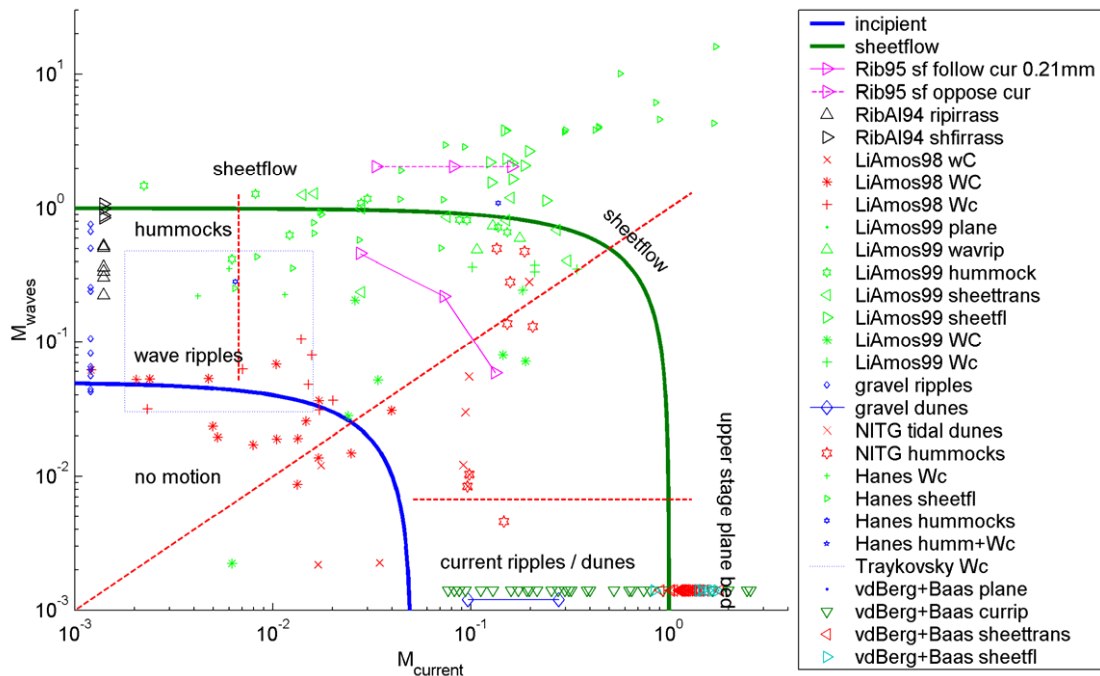


Figure 2 Normalised bed state diagram based on rational criteria for beginning of motion and sheetflow/UPB

Normalised to remove the grain size influence on the criteria. The dotted box indicates the position of the Traykovski *et al.* (1999) data which contains incipient motion (bottom), 2D and 3D wave ripples modified by a small current. Experimental current ripple data in silt and sands are of Van den Berg and Van Gelder (1993), and Baas (1994, 1999), Baas and de Koning (1995). *Reproduced from Kleinhans (2005) with permission.*

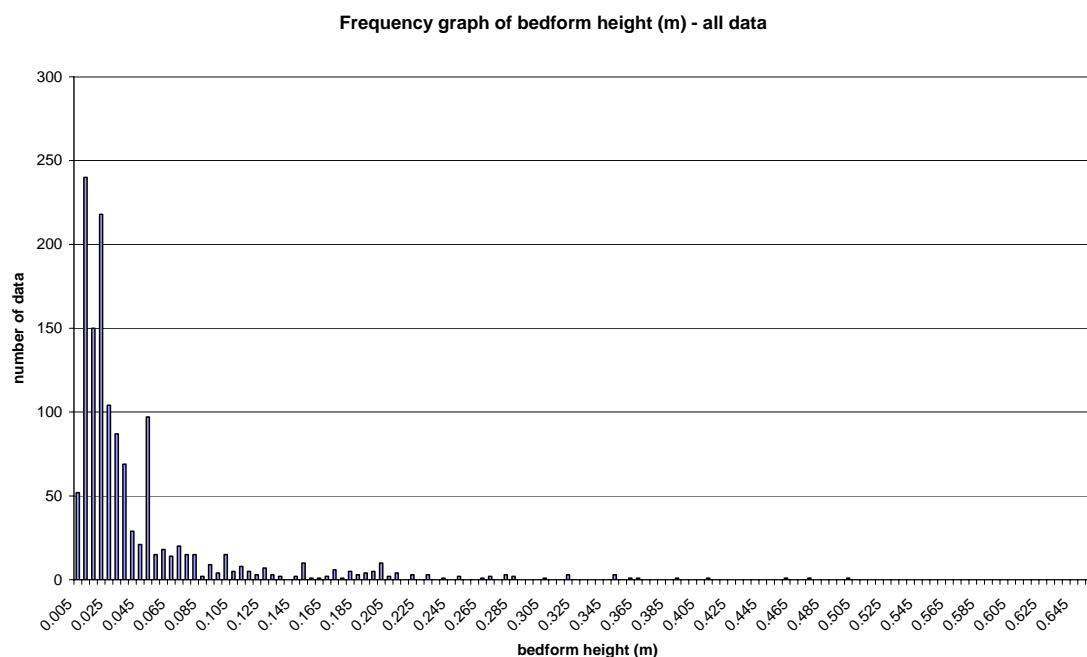


Figure 3 Frequency distribution of *all* ripple heights

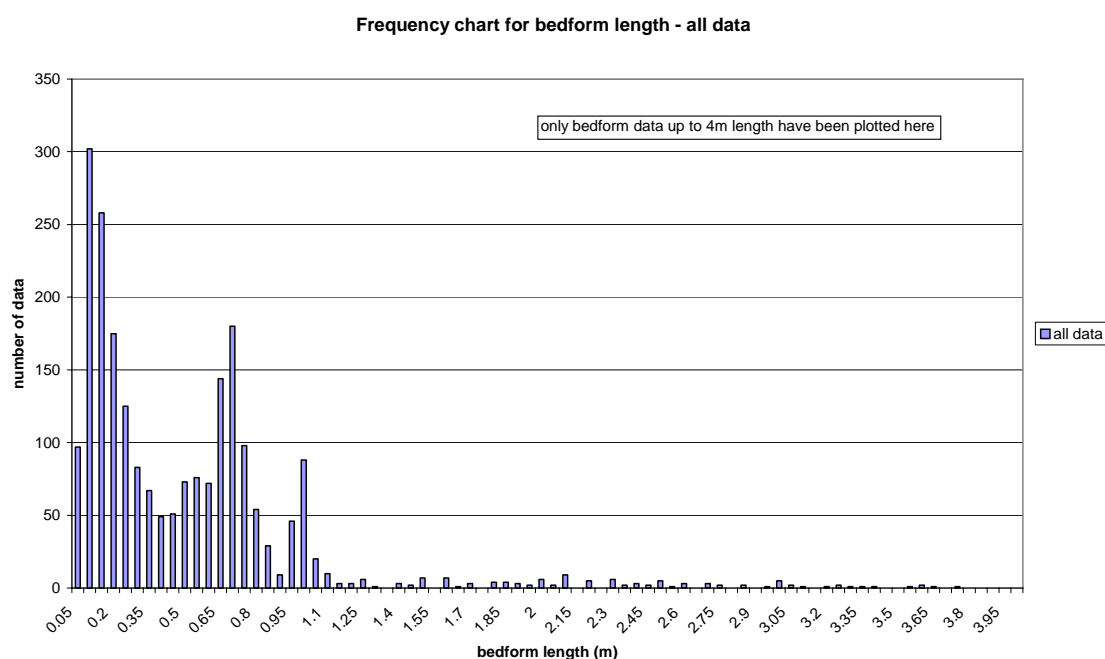


Figure 4 Frequency distribution of *all* ripple wavelengths < 4m

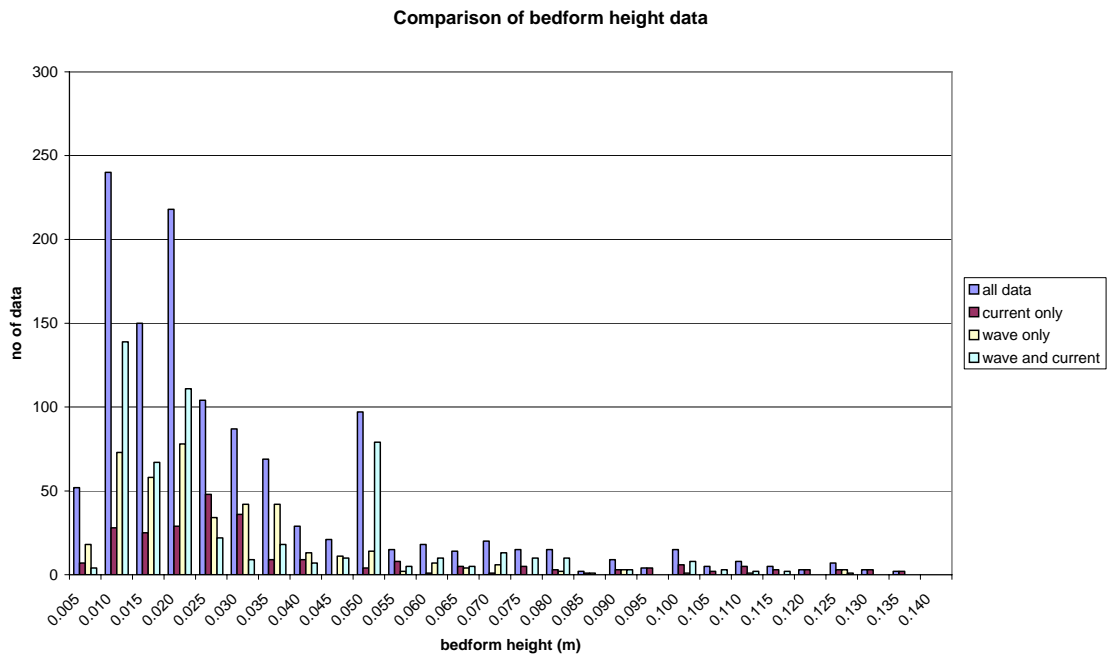


Figure 5 Frequency distribution of ripple heights subdivided into flow classes

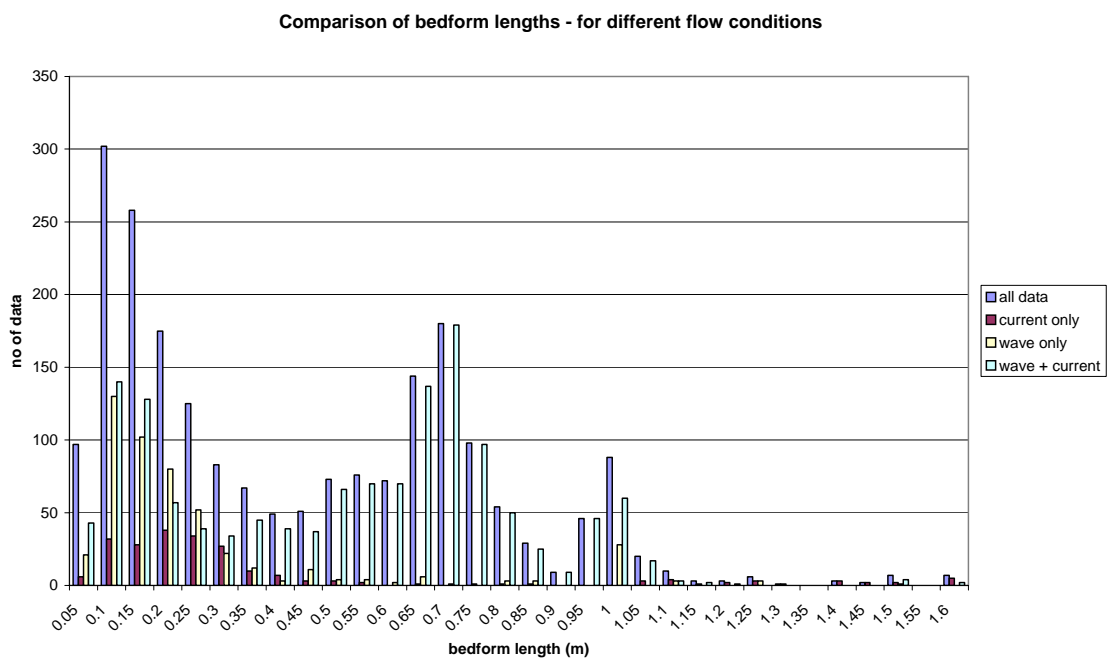


Figure 6 Frequency distribution of ripple wavelengths (< 4m) subdivided into flow classes

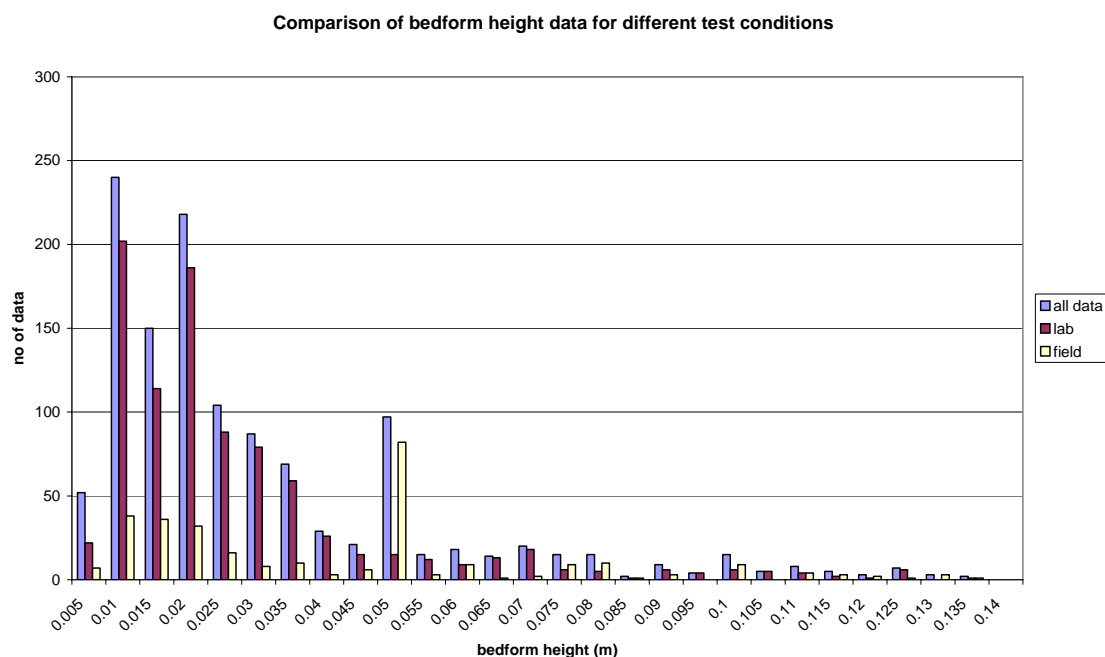


Figure 7 Frequency distribution of ripple heights subdivided into lab and field experiments

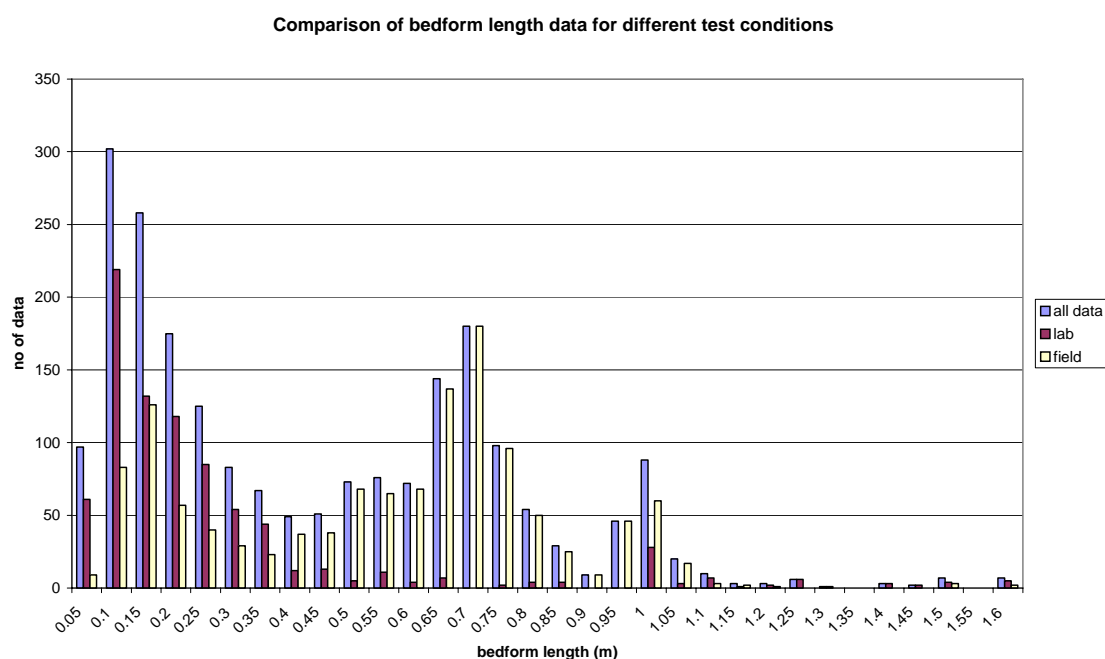


Figure 8 Frequency distribution of ripple wavelengths (< 4m) subdivided into lab and field experiments

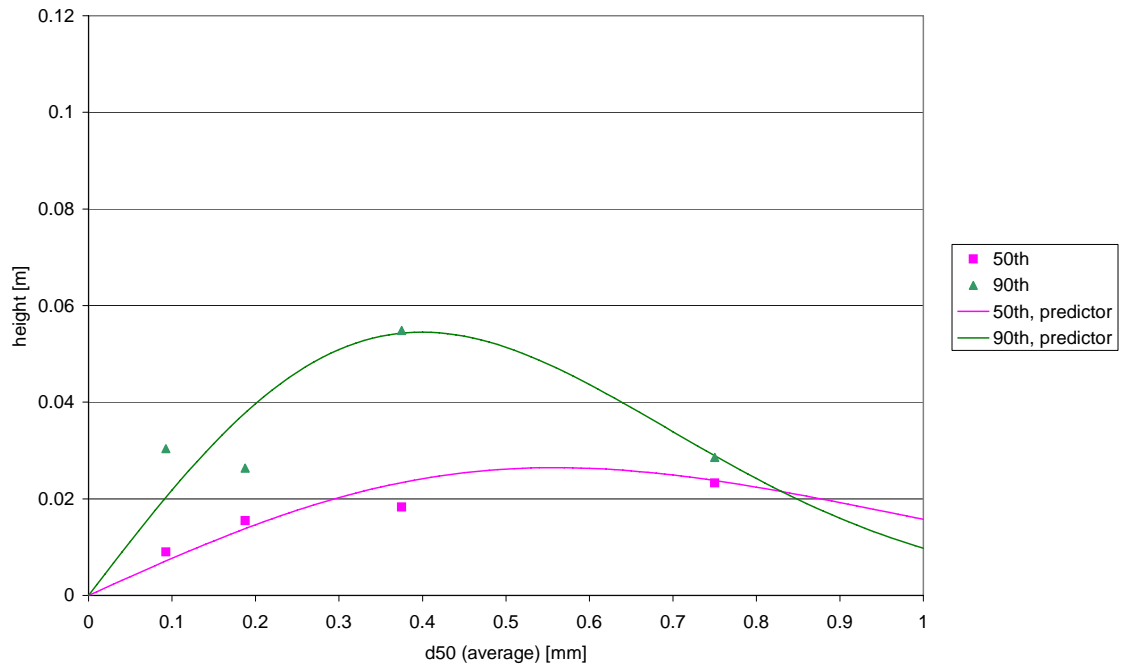


Figure 9 50 and 90-percentile ripple heights for currents, with fitted prediction curves

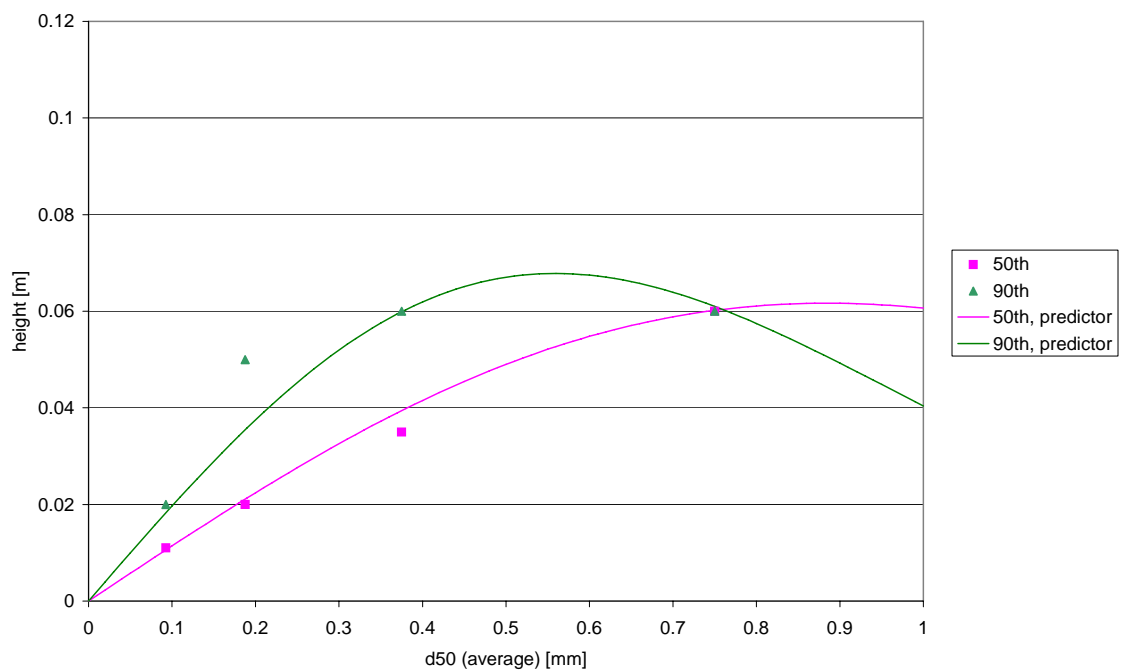


Figure 10 50 and 90-percentile ripple heights for waves, with fitted prediction curves

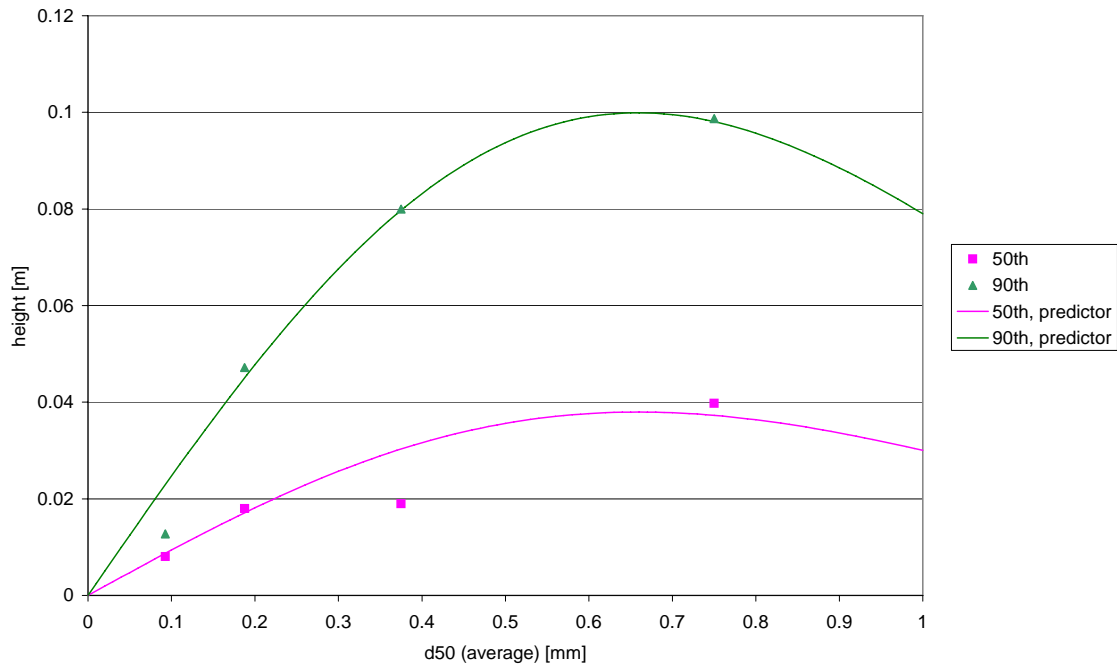


Figure 11 50 and 90-percentile ripple heights for W + C, with fitted prediction curves

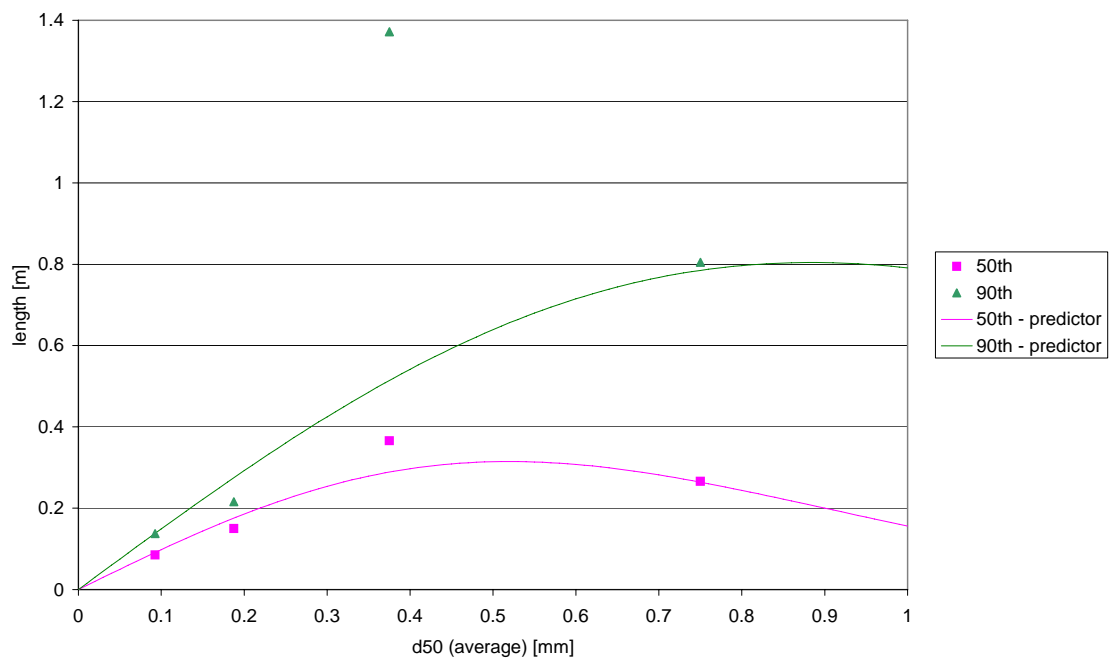


Figure 12 50 and 90-percentile ripple wavelengths (< 1.5m) for currents, with fitted prediction curves

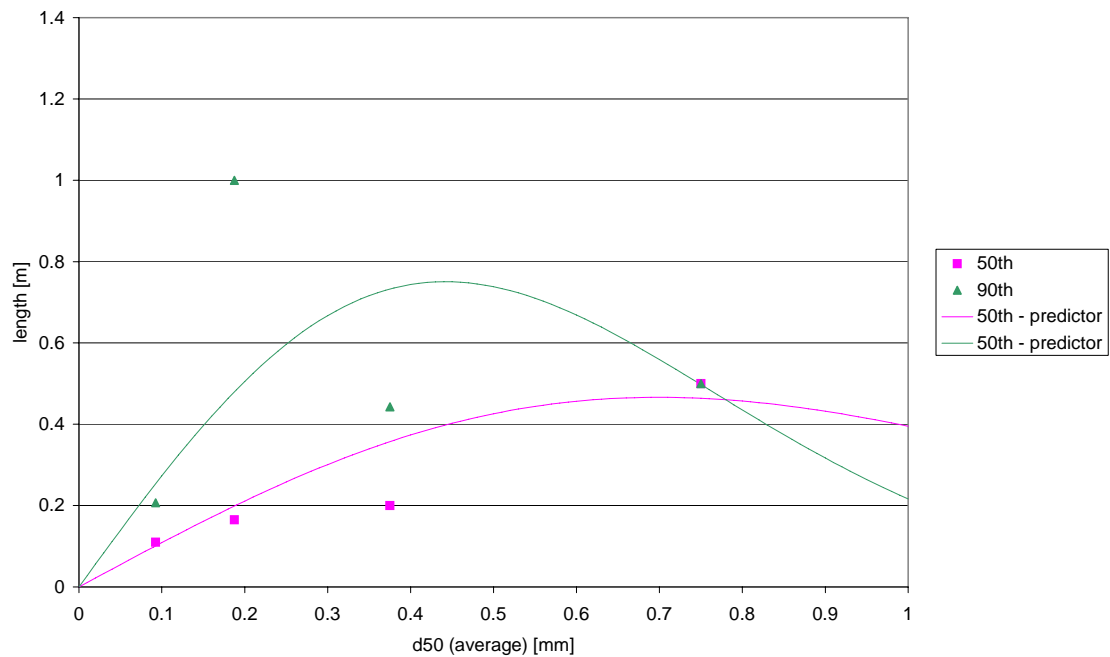


Figure 13 50 and 90-percentile ripple wavelengths (< 1.5m) for waves, with fitted prediction curves

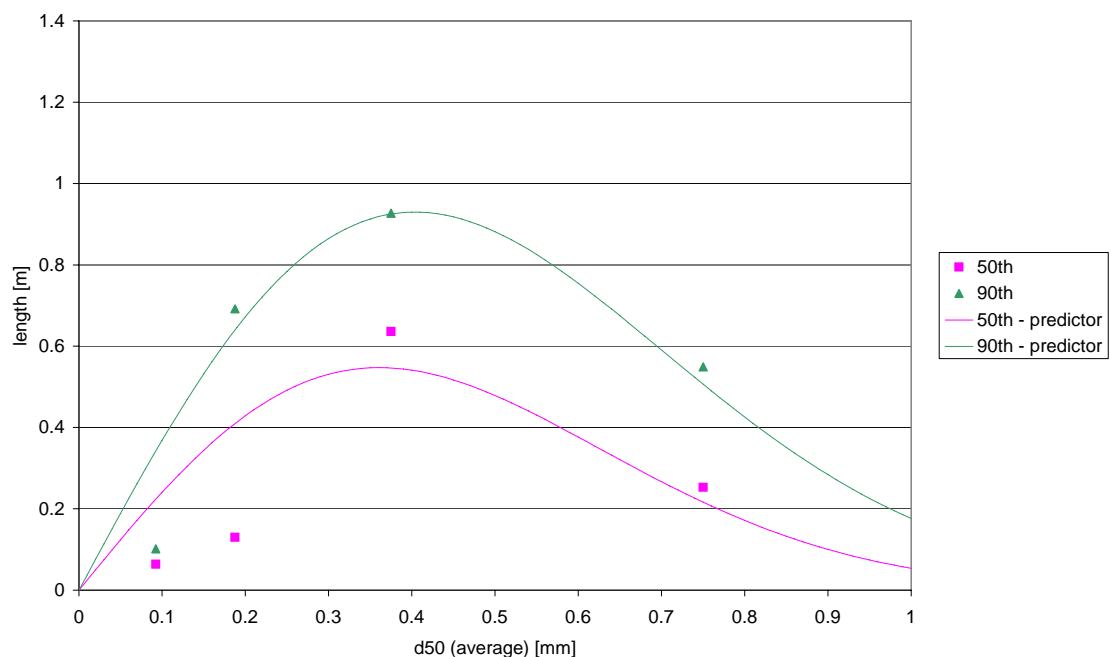


Figure 14 50 and 90-percentile ripple wavelengths (< 1.5m) for W + C, with fitted prediction curves

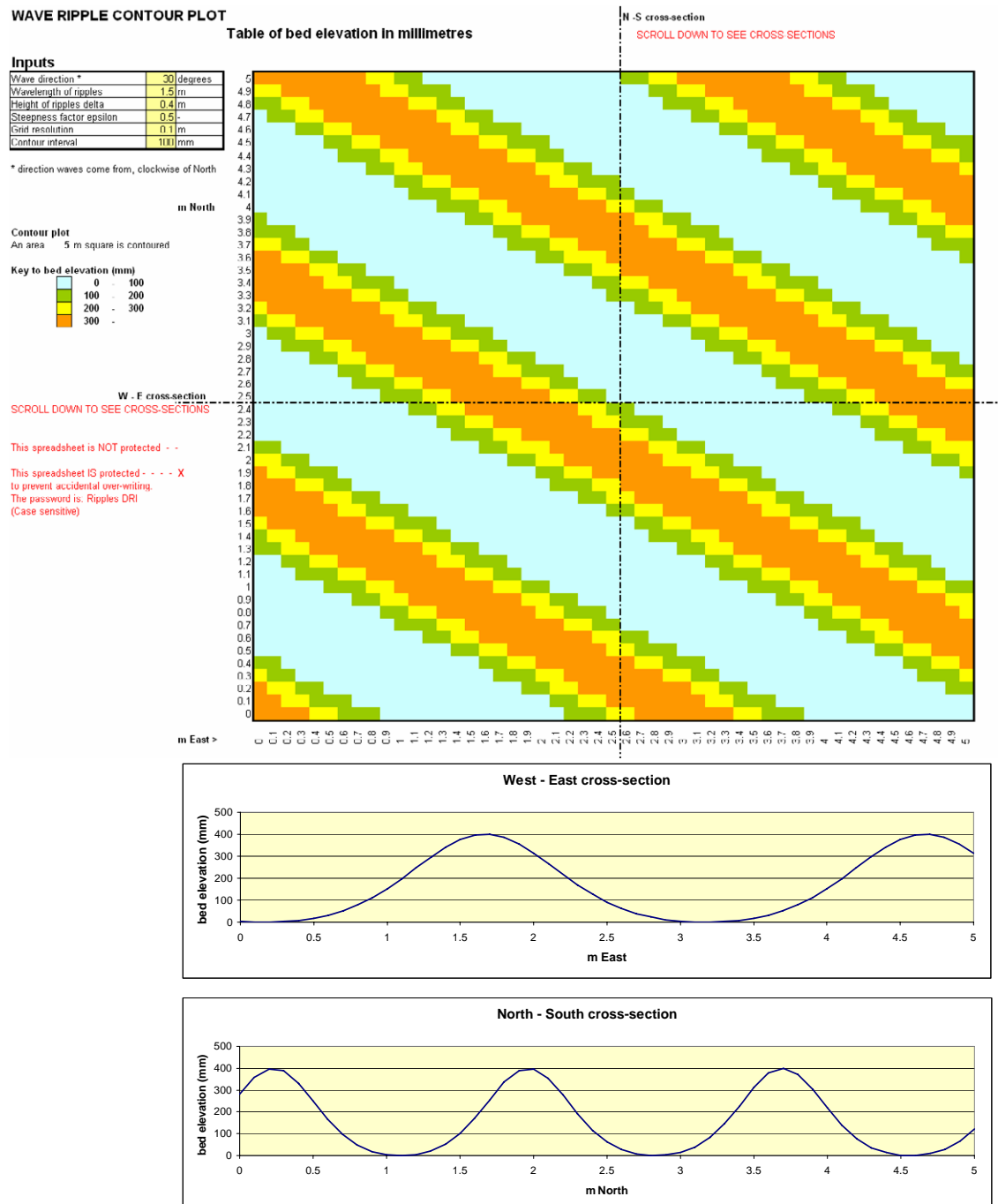


Figure 15 Example of contour plot of bed elevation and cross-sections of wave-generated ripples for wave direction 30° , ripple wavelength 1.5m, ripple height 0.4m, sharpness factor = 0.5

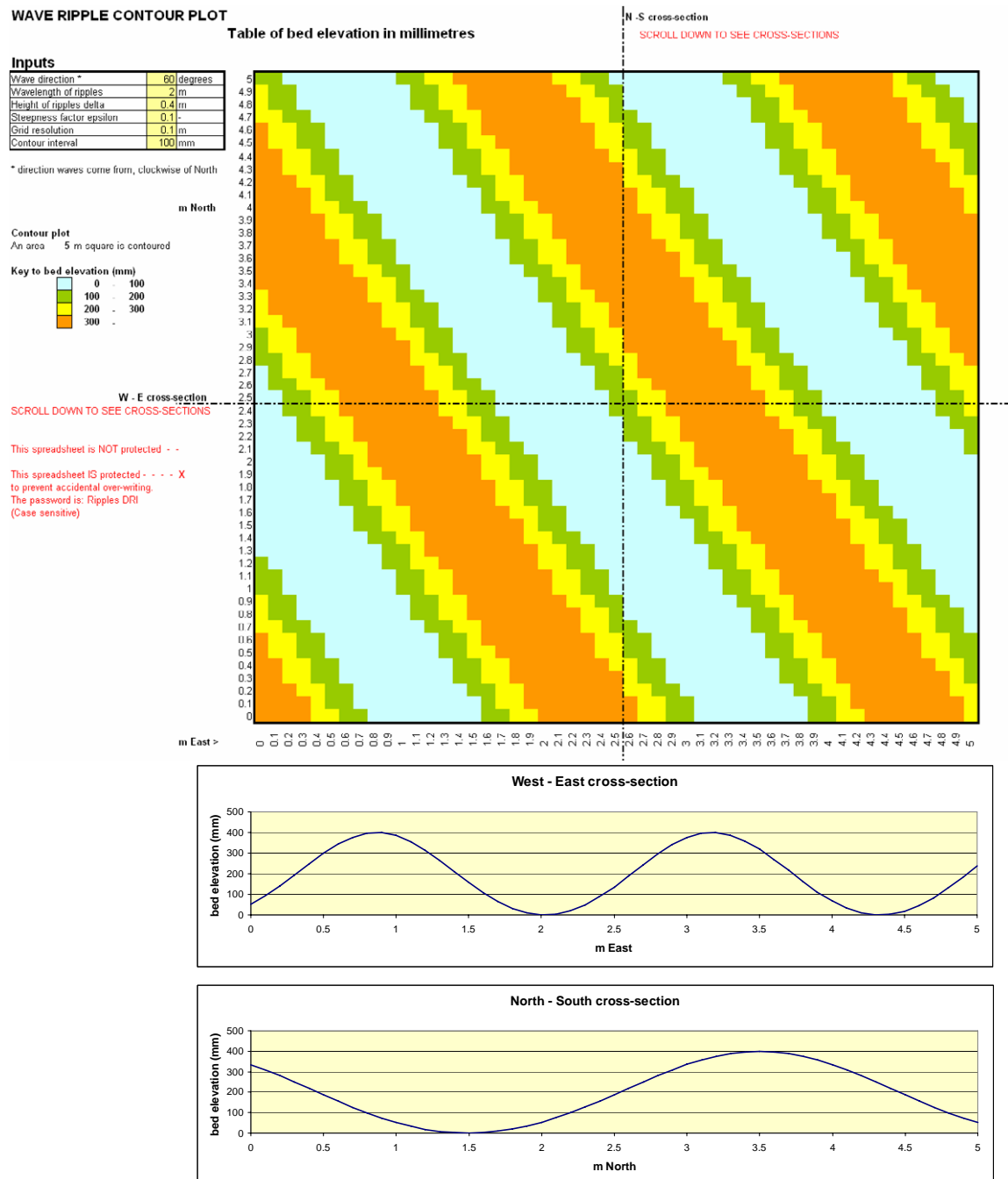


Figure 16 Example of contour plot of bed elevation and cross-sections of wave-generated ripples for wave direction 60°, ripple wavelength 2m, ripple height 0.4m, sharpness factor = 0.1

